Behavioral/Cognitive

Prefrontal $GABA_A(\delta)R$ Promotes Fear Extinction through Enabling the Plastic Regulation of Neuronal Intrinsic Excitability

Han-Qing Pan,[1,2] Xiao-Xuan Liu,[1,4] Ye He,[3] Jin Zhou,[2] Cai-Zhi Liao,[1,2] Wen-Jie You,[1,2] Si-Ying Jiang,[1,2] Xia Qin,[1,2,5] Wen-Bing Chen,[1,2] Er-Kang Fei,[1,2] Wen-Hua Zhang,[1,2] and Bing-Xing Pan[1,2]

[1]Laboratory of Fear and Anxiety Disorders, Institutes of Life Science, Nanchang University, Nanchang 330031, People's Republic of China, [2]Department of Biological Science, School of Life Sciences, Nanchang University, Nanchang 330031, People's Republic of China, [3]Center for Medical Experiments, Nanchang University, Nanchang 330031, People's Republic of China, [4]Neurology Department, The Second Xiangya Hospital, Central South University, Changsha 410011, People's Republic of China, and [5]Jiangsu Provincial Key Laboratory of Anesthesiology, Xuzhou Medical University, Xuzhou 221004, People's Republic of China

Extinguishing the previously acquired fear is critical for the adaptation of an organism to the ever-changing environment, a process requiring the engagement of $GABA_A$ receptors ($GABA_A$Rs). $GABA_A$Rs consist of tens of structurally, pharmacologically, and functionally heterogeneous subtypes. However, the specific roles of these subtypes in fear extinction remain largely unexplored. Here, we observed that in the medial prefrontal cortex (mPFC), a core region for mood regulation, the extrasynaptically situated, δ-subunit-containing $GABA_A$Rs [$GABA_A(\delta)$Rs], had a permissive role in tuning fear extinction in male mice, an effect sharply contrasting to the established but suppressive role by the whole $GABA_A$R family. First, the fear extinction in individual mice was positively correlated with the level of $GABA_A(\delta)$R expression and function in their mPFC. Second, knockdown of $GABA_A(\delta)$R in mPFC, specifically in its infralimbic (IL) subregion, sufficed to impair the fear extinction in mice. Third, $GABA_A(\delta)$R-deficient mice also showed fear extinction deficits, and re-expressing $GABA_A(\delta)$Rs in the IL of these mice rescued the impaired extinction. Further mechanistic studies demonstrated that the permissive effect of $GABA_A(\delta)$R was associated with its role in enabling the extinction-evoked plastic regulation of neuronal excitability in IL projection neurons. By contrast, $GABA_A(\delta)$R had little influence on the extinction-evoked plasticity of glutamatergic transmission in these cells. Altogether, our findings revealed an unconventional and permissive role of extrasynaptic $GABA_A$ receptors in fear extinction through a route relying on nonsynaptic plasticity.

Key words: **excitability; fear extinction; $GABA_A$(d)R; medial prefrontal cortex; plasticity**

Significance Statement

The medial prefrontal cortex (mPFC) is one of the kernel brain regions engaged in fear extinction. Previous studies have repetitively shown that the $GABA_A$ receptor ($GABA_A$R) family in this region act to suppress fear extinction. However, the roles of specific $GABA_A$R subtypes in mPFC are largely unknown. We observed that the $GABA_A$R-containing δ-subunit [$GABA_A(\delta)$R], a subtype of $GABA_A$Rs exclusively situated in the extrasynaptic membrane and mediating the tonic neuronal inhibition, works oppositely to the whole $GABA_A$R family and promotes (but does not suppress) fear extinction. More interestingly, in striking contrast to the synaptic $GABA_A$Rs that suppress fear extinction by breaking the extinction-evoked plasticity of glutamatergic transmission, the $GABA_A(\delta)$R promotes fear extinction through enabling the plastic regulation of neuronal excitability in the infralimbic subregion of mPFC. Our findings thus reveal an unconventional role of $GABA_A(\delta)$R in promoting fear extinction through a route relying on nonsynaptic plasticity.

Received Apr. 4, 2022; revised June 2, 2022; accepted June 6, 2022.

Author contributions: H.-Q.P. and B.-X.P. designed research; H.-Q.P., X.-X.L., Y.H., J.Z., C.-Z.L., W.-J.Y., S.-Y.J., and W.-B.C. performed research; H.-Q.P., X.-X.L., Y.H., C.-Z.L., W.-J.Y., S.-Y.J., X.Q., and W.-B.C. contributed unpublished reagents/analytic tools; H.-Q.P., X.-X.L., Y.H., J.Z., C.-Z.L., W.-J.Y., and X.Q. analyzed data; H.-Q.P., E.-K.F., W.-H.Z., and B.-X.P. wrote the paper.

This work was supported by the National Key R&D Program of China (Grant 2021ZD0202704), the National Natural Science Foundation of China (Grants 82125010, 81930032, 31970953, 32160193, and 81771459), and the Natural Science Foundation of Jiangxi Province (Grants 20172BCB22005, 20192ACB20023, and 20212ACB206038).

The authors declare no competing financial interests.

Correspondence should be addressed to Bing-Xing Pan at panbingxing@ncu.edu.cn.

https://doi.org/10.1523/JNEUROSCI.0689-22.2022

Introduction

Extinction of the previously learned, threat-related fear in the absence of threat, a process called fear extinction, is essential for an individual's adaptation to the constantly changing environment (Tovote et al., 2015). The insufficiency or failure of fear extinction has been implicated in the development of a spectrum of neuropsychological diseases, including post-traumatic stress disorder (PTSD) and anxiety disorders (Myers and Davis, 2007; Bisson et al., 2015). Both animal and human studies have consistently implicated the medial prefrontal cortex (mPFC) as one of the kernel brain regions for the encoding and expression of extinction memories (Etkin et al., 2011; Giustino and Maren, 2015). In rodents, mPFC lesions have been shown to impair the fear extinction (Morgan et al., 1993; Quirk et al., 2000). And, pharmacologically or optogenetically manipulating the neuronal activity within the mPFC is sufficient to change the ability of the rodents to extinguish the learned fear (Corcoran and Quirk, 2007; Sierra-Mercado et al., 2011; Marek et al., 2018a,b). In humans, fMRI data revealed a positive correlation between ventromedial PFC (vmPFC) activation and the degree of extinction memory recall (Milad et al., 2007), and that the PTSD patients were found to fail to activate vmPFC when exposed to cues promoting extinction (Milad et al., 2009).

The mPFC engagement in fear extinction requires the dynamic interplay of a spectrum of neurotransmitters and neuromodulators (Bukalo et al., 2014). Among these, the inhibitory signals mediated by the GABA transmitter and its receptors are generally thought to suppress the extinction of learned fear (Davis and Myers, 2002; Chhatwal et al., 2005; Sierra-Mercado et al., 2011; Marek et al., 2018a; Chen et al., 2022). It was shown that chemogenetically activating the parvalbumin-positive interneurons in the infralimbic (IL) subregion of mPFC diminishes the fear extinction recall (Marek et al., 2018a; Chen et al., 2022). Moreover, microinjecting the nonselective $GABA_A$ receptor ($GABA_AR$) agonist muscimol into the IL before extinction training results in an impairment of both acquisition and retention of extinction memory (Sierra-Mercado et al., 2011). As the primary mediators of GABAergic signals in the brain, the $GABA_AR$ family is composed of tens of members that differ in their subunit composition, pharmacological properties, subcellular localization, and physiological function. It remains largely unexplored how specific $GABA_AR$ subtypes in mPFC are engaged in the regulation of fear extinction.

Here, by screening the expression of different $GABA_AR$ subunits in the mPFC of mice with variable fear extinction, we observed that, among the diverse $GABA_AR$ subtypes, the $GABA_AR$ containing the δ-subunit [$GABA_A(\delta)R$] in mPFC arose to signal the ability of individual mice to extinguish the learned fear. Somewhat surprisingly, the $GABA_A(\delta)R$ acted to promote the extinction of learned fear, an effect sharply contrasting to the established but suppressive role of the $GABA_AR$ family in tuning fear extinction. We further observed that the permissive role of $GABA_A(\delta)R$ was associated with its role in enabling the extinction-evoked plastic regulation of excitability of IL neurons.

Materials and Methods

Animals. C57BL/6J mice (stock #N000013) and *Gabrd* KO mice (stock #003725) were initially purchased from the Model Animal Research Center of Nanjing University (Nanjing, People's Republic of China) and The Jackson Laboratory, respectively, and bred in the temperature-fixed, humidity-controlled animal colony with a 12 h light/dark circle (7:00 A.M. to 7:00 P.M.) in Nanchang University. The animals were weaned and genotyped at postnatal day 21 (P21). Three to five experimentally used male mice were kept in the same cage with free access to food and water. All experiments were under the guidance of the Institutional Animal Care and Use Committee of Nanchang University.

Fear conditioning and extinction. The mice were trained with a 5 d procedure including the habituation, fear learning, first extinction (first Ext), second extinction (second Ext), and memory retention test by a Video Freeze system (MED-VFC-SCT-M, Med Associates). For the habituation process, the mice were placed in Context A (white room light, ON state of chamber light, 4% acetic acid, uncovered stimulation steel, ON state of background noise) for 180 s and then were presented with five conditioned stimuli (CSs; a 20 s, 3 kHz tone with an intensity of 80 dB at variable intervals of 50–80 s). Thirty seconds after the last CS, the mice were taken back to their home cages. Twenty-four hours later, the fear-learning process was performed. The unconditioned stimulus (US) was a 1 s, 1.0 mA electric shock coterminated with the CS. The mice were returned to Context A for 180 s and received five CS–US pairings with variable intervals (50–150 s). Thirty seconds after the last CS–US pairing was given, the mice were brought back to their home cages. Twenty-four hours after fear learning, the mice were trained with 2 consecutive days of fear extinction. For fear extinction, the mice were placed in Context B (red room light, OFF state of chamber light, 75% ethanol, stimulation steel covered with a plastic plate, OFF state of background noise) and 10 CSs were presented at different intervals of 40–90 s for each extinction session were given. Twenty-four hours after the second Ext, the mice were placed in Context B again and received two CSs at a 73 s interval. The fear responses were scored as the immobile time spent during CS and analyzed by Video Freeze (Med Associates).

The calculations of extinction retention index (ERI) and extinction learning index (ELI) were referred to the method by Milad et al. (2008) with minor modifications. Briefly, the average freezing levels for the last two CSs of the second Ext Phase, and for the CS during the Test Phase, were subtracted from the average freezing percentage for the first two CSs during the first Ext Phase. These two values were divided by the freezing percentage and multiplied by 100, yielding the ELI and ERI, respectively.

c-Fos immunostaining. The mice were deeply anesthetized and perfused transcardially with 0.1 M PBS and 4% paraformaldehyde (PFA). The brains were removed and postfixed in PFA overnight. Coronal sections (40 μm thick) containing IL were sectioned using a vibrating slicer (model VT1000S Vibratome, Leica Microsystems). The sections were incubated in the blocking buffer (10% donkey serum dissolved in the PBS-Triton X-100) at room temperature for 2 h, then incubated in the primary antibody against c-*Fos* (1:500; rabbit anti-mouse, Santa Cruz Biotechnology) overnight at 4°C. Then, the sections were incubated with fluorescent secondary antibody (1:500; donkey anti-rabbit, Alexa Fluor 568, Thermo Fisher Scientific) at room temperature for 2 h. DAPI (Beyotime Institute of Biotechnology) was added into the incubation buffer for 5 min, then the sections were mounted on the glass slide and coverslipped with the Fluoromount Aqueous Mounting Medium (Sigma-Aldrich). Microscopy inspection was performed by a laser-scanning confocal microscope (model FV1000, Olympus), and the quantification of c-*Fos* numbers was achieved by ImageJ software (National Institutes of Health) as we described previously (Zhang et al., 2019).

Electrophysiology. Electrophysiological recordings were performed as previously described (Pan et al., 2020). Briefly, the mice were anesthetized with ether and decapitated. The brains were removed quickly and chilled in the ice-cold, bubbled (95% O_2/5% CO_2) partial sucrose artificial CSF (ACSF) containing the following (in mM): 80 NaCl, 3.5 KCl, 4.5 $MgSO_4$, 0.5 $CaCl_2$, 1.25 $NaH_2PO_4 \cdot 2H_2O$, 25 $NaHCO_3$, 10 glucose, and 90 sucrose, at pH 7.3–7.4. The coronal slices (320 μm thick) including mPFC or basolateral amygdala (BLA) were collected by a vibrating slicer (VT1000S Vibratome, Leica Microsystems) and moved to the prewarmed (34°C) ACSF containing the following (in mM): 124 NaCl, 2.5 KCl, 1 $MgSO_4$, 2.5 $CaCl_2$, 1.25 $NaH_2PO_4 \cdot 2H_2O$, 25 $NaHCO_3$, and 10 glucose, pH 7.3–7.4, for 30 min. Then the slices were incubated at room temperature for at least 1 h before recordings.

Table 1. Sequences of the primers used in qRT-PCR

Gene	Direction	Sequence
Gabra1	Forward	5′-AAAAGTCGGGGTCTCTCTGAC-3′
	Reverse	5′-CAGTCGGTCCAAAATTCTTGTGA-3′
Gabra2	Forward	5′-AGAAAAACCCTCTTCTTCGGATG-3′
	Reverse	5′-GTGGCATTGTTCATTTGAATGGT-3′
Gabra3	Forward	5′-ATGGGCACTTTTATGTGACCA-3′
	Reverse	5′-CCCCAGGTTCTTGTCGTCTTG-3′
Gabra4	Forward	5′-ACAATGAGACTCACCATAAGTGC-3′
	Reverse	5′-GGCCTTTGGTCCAGGTGTAG-3′
Gabra5	Forward	5′-TGACCCAAACCCTCCTTGTCT-3′
	Reverse	5′-GTGATGTTGTCATTGGTCTCGT-3′
Gabrb1	Forward	5′-TCCCGTGATGGTTGCTATGG-3′
	Reverse	5′-CCGCAAGCGAATGTCATATCC-3′
Gabrb2	Forward	5′-ATGTCGCTGGTTAA AGAGACG-3′
	Reverse	5′-CTGCCACTCGGTTGTCCAAA-3′
Gabrb3	Forward	5′-CACGCTTGACAATCGAGTGG-3′
	Reverse	5′-GCGGATCATGCGGTTTTTCAC-3′
Gabrg2	Forward	5′-AGAAAAACCCTCTTCTTCGGATG-3′
	Reverse	5′-GTGGCATTGTTCATTTGAATGGT-3′
Gabrd	Forward	5′-ATTGGGGACTACGTGGGCT-3′
	Reverse	5′-CCACATTCACAGGAGCACC-3′
Gabrr1	Forward	5′-CGAGGAGCACACGACGATG-3′
	Reverse	5′-GTGAAGTCCATGTCAACCTCTG-3′
Gapdh	Forward	5′-AGGTCGGTGTGAACGGATTTG-3′
	Reverse	5′-TGTAGACCATGTAGTTGAGGTCA-3′

The slices were transferred to the recording chamber and perfused with ACSF at a rate of 2 ml/min. The temperature of perfusion solution was maintained at 30 ± 1°C by a temperature controller (TC-324B, Warner Instrument). The whole-cell recording was performed in all electrophysiological experiments, and the data were obtained by Axon 700B Amplifier and Digidata 1440A digital-analog convertor (Molecular Devices). The sampling frequency and filter frequency were set at 10 and 3 kHz, respectively.

To record GABAergic currents, an intraelectrode solution was used containing the following (in mM): 100 CsCl, 30 Cs-methane sulfonate, 5 KCl, 2 $MgCl_2$, 10 HEPES, 0.2 EGTA, 2 ATP-Mg, 0.1 GTP-Na, and 5 QX-314, at pH 7.3–7.4 and 290 mOsm. The perfusion ACSF had 20 μM CNQX, 50 μM DL-APV, and 5 μM CGP52432 added to block ionic glutamatergic and $GABA_BR$-mediated currents, and cells were held at −70 mV in voltage-clamp mode. The spontaneous IPSCs (sIPSCs) and tonic inhibitory currents were acquired simultaneously. After 2–3 min of sIPSC recording, 2 μM tetrahydroisoxazolopyridinol (THIP) was applied in the perfusate for 5 min to fully activate extrasynaptic $GABA_ARs$. The augmented holding current mediated by THIP was defined as THIP-evoked current. To record miniature IPSCs (mIPSCs), 1 μM TTX was additionally included in the perfusate to block action potential.

In measuring of neuronal excitability and miniature EPSCs (mEPSCs), the following intraelectrode solution containing was used (in mM): 130 K-gluconate, 5 KCl, 2 $MgCl_2$, 10 HEPES, 0.2 EGTA, 2 ATP-Mg, and 0.1 GTP-Na, at pH 7.3–7.4 and 290 mOsm. To record the action potentials, the patched neurons were held at −70 mV in the current-clamp mode. A serial number of depolarization currents ranging from 50 to 250 pA in 50 pA intervals was injected into the cells. To record mEPSCs, the voltage-clamp mode was performed, with 100 μM picrotoxin (PTX), 5 μM CGP52432, and 1 μM TTX dissolved in the bath solution.

To recorded paired-pulse ratio (PPR) of EPSCs, a concentric bipolar stimulating electrode (FHC) was placed in layer II/III, and the voltage-clamp recordings were performed in layer V neurons. The following intraelectrode solution was used (in mM): 130 Cs-methanesulfonate, 5 NaCl, 1 MgCl2, 10 HEPES, 0.2 EGTA, 2 ATP-Mg, 0.1 GTP-Na, 5 QX-314, at pH 7.3–7.4 and 290 mOsm, and 100 μM PTX was perfused to the slices. To record the PPR, the patched cells were clamped at −70 mV, and two electrical stimuli were delivered at 50 ms intervals. The stimulation intensity was adjusted to make the first evoked EPSC at 50–150 pA. In all electrophysiological experiments, the pipette resistance was at 2–7 MΩ, and series resistance (R_s) was at 10–20 MΩ. The R_s was monitored before and after the experiments, and if the variation in R_s values was >20%, the data would be discarded. The neuronal excitability, PPRs were analyzed using Clampfit (Molecular Devices); the analysis of sIPSCs, mIPSCs, and mEPSCs were performed using Mini Analysis (Synaptosoft); and the analysis of THIP-evoked current was achieved using Origin (Microcal).

Table 2. Sequences of shRNAs targeting *Gabrd* are provided as below

Name of shRNA	Sequence
shRNA1(*Gabrd*)	CCAGGGCAATGAATGACAT
shRNA2(*Gabrd*)	CCACGGAGCTGATGAACTT
shRNA3(*Gabrd*)	GGAAGAAACGGAAAGCCAA

Transcriptional analysis of $GABA_AR$ subunits. Quantitative real-time PCR (qRT-PCR) was performed to analyze the transcriptional profile of the $GABA_AR$ subunits. The 500 μm coronal sections containing mPFC and BLA were obtained as described in the electrophysiological assay. The bilateral mPFC and BLA tissue was microdissected under the dissecting microscope (Leica Microsystems). The RNA was subsequently extracted using TRIzol (Thermo Fisher Scientific), and reverse transcription was performed using the RevertAid RT Kit (Thermo Fisher Scientific) according to the manufacturer instructions. qRT-PCR was conducted using SYBR Green PCR Master Mix (Thermo Fisher Scientific) on a StepOne Real-Time PCR System (Thermo Fisher Scientific). Each sample was tested in triplicate. GAPDH mRNA quantification was used as a loading control for normalization. Fold changes of mRNA levels over controls were analyzed using the $2\text{-}\Delta\Delta C_T$ method. Sequences of the primers used in qRT-PCR are listed in Table 1.

Western blot. The process of Western blot was as previously described (Zheng et al., 2021). Briefly, mPFC tissue was microdissected as described above. The tissue was ultrasonicated and homogenized in ice-cold PBS plus protease inhibitors and lysed in 2× radioimmunoprecipitation assay buffer [0.2% SDS (w/v), 1% sodium deoxycholate (w/v), and 2% Nonidet P-40 (v/v) in PBS] with protease inhibitors. After centrifuging at 700 × *g* at 4°C for 10 min, the supernatant was collected, and the total protein concentration was quantified by a bicinchoninic acid protein kit (Beyotime Institute of Biotechnology). Proteins of ~20 μg were subjected to SDS-PAGE. They then were transferred to polyvinylidene fluoride membrane (Millipore) and blocked with 5% nonfat milk for 2 h at room temperature. The membranes were then incubated with the primary antibodies (1:1000; anti-δ-subunit of $GABA_AR$, rabbit anti-mouse, R&D Systems; 1:5000; anti β-actin, rabbit anti-mouse, Proteintech) overnight followed by incubation with secondary antibody for 1 h at room temperature. The immunoreactive bands were visualized by enhanced chemiluminescence (Thermo Fisher Scientific), and the images were captured by fluorescent spectral imager (BIO-RAD). The integrated gray values were analyzed by the ImageJ software (National Institutes of Health).

Stereotaxic surgery. The P35 to P42 male mice were used for stereotaxic surgery (Liu et al., 2020). Briefly, the mice were anesthetized with 2% (w/v) pentobarbital sodium and positioned in a stereotaxic frame (RWD), and the body temperature was maintained with a heating pad. Their eyes were lubricated with an ophthalmic ointment to avoid corneal drying. The scalp of the mice undergoing surgery was dissected along the midline to expose the skull. The target site was defined using stereotactic coordinates. The coordinates relative to bregma were as follows: prelimbic (PL) subregion: anteroposterior (AP), +1.94 mm; mediolateral (ML), ±0.25 mm; dorsoventral (DV), −1.95 mm; IL subregion: AP, +1.80 mm; ML, ±0.25 mm; DV, −2.90 mm. All the viruses were diluted to 1.0×10^{12} infectious particles/ml and were delivered into the target brain area by a calibrated glass microelectrode mounted on a Microliter syringe (Hamilton) at a rate of 30 nl/min under a microsyringe pump (Stoelting). To knock down the *Gabrd* expression, the AAV-*CMV*-bGlobin-EGFP-H1-shRNA1(*Gabrd*)-H1-shRNA2(*Gabrd*)-H1-shRNA3 (*Gabrd*) or the control virus (AAV-*CMV*-bGlobin-EGFP-H1-shRNA) was bilaterally delivered into the PL or IL subregion (0.2 μl/hemisphere) of WT mice, the sequences of shRNAs targeting *Gabrd* are provided as below (Table 2).

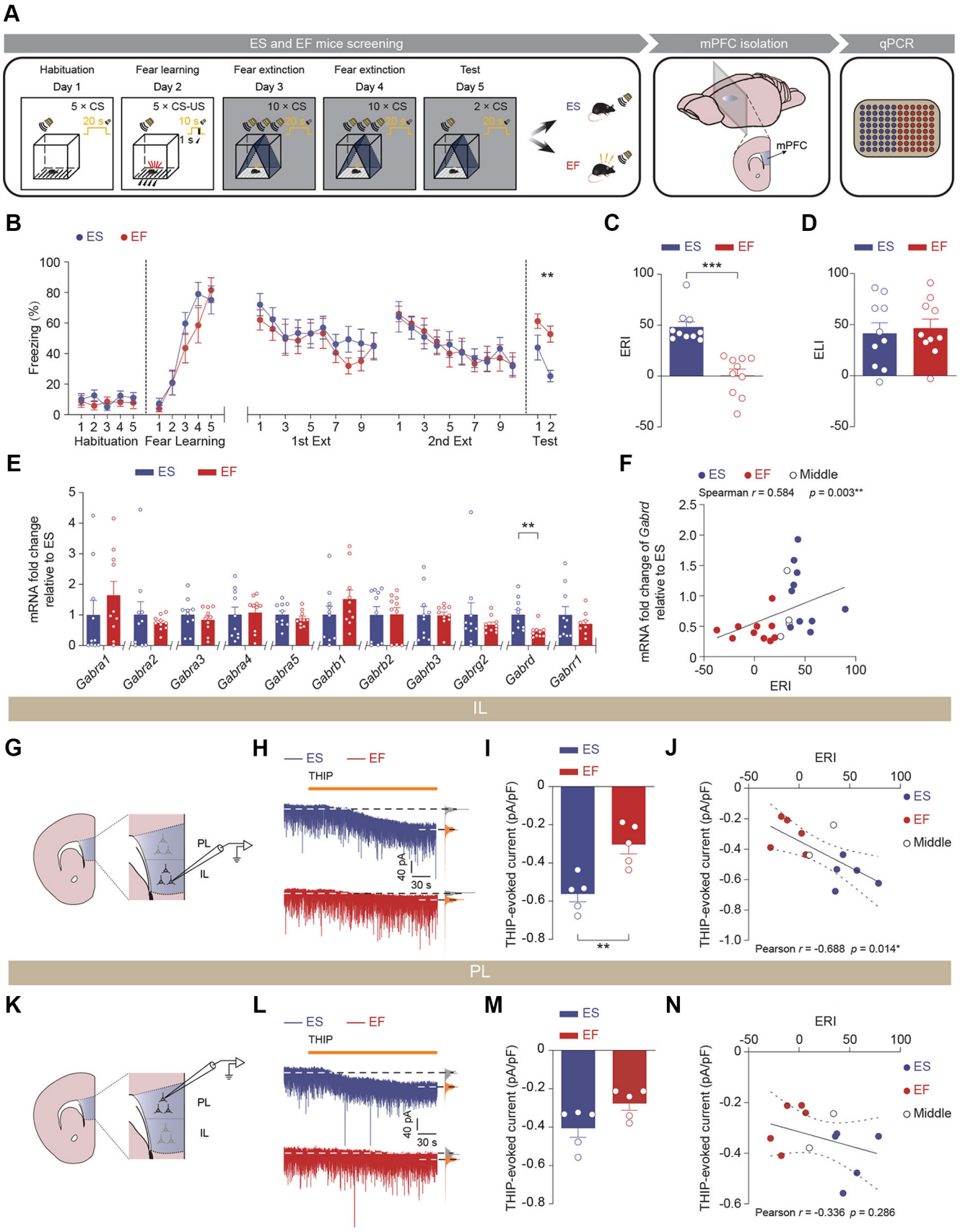

Figure 1. Correlation of GABA$_A$(δ)R expression and function in the IL subregion with fear extinction in mice. ***A***, Schematic illustration of fear conditioning and extinction paradigms for the screening of ES and EF mice, and sequential mPFC isolation and quantitative PCR tests. ***B***, The freezing levels of ES and EF mice in response to tones (CS) alone or paired with footshocks (US) as indicated in ***A*** during habituation, fear learning, Ext, and Test sessions. The ERI for each mouse was calculated, and mice within the top or bottom 40% of ERI were designated as ES or EF, respectively. ES, $n = 10$ mice; EF, $n = 10$ mice, comparisons were performed between ES and EF mice. ***C***, Comparisons of ERI between EF and ES mice. Same sample size as in ***B***. ***D***,

To re-express *Gabrd*, AAV-*SYN*-*Gabrd*-2A-EGFP-3×FLAG or the control virus (AAV-*SYN*-EGFP-3×FLAG) was bilaterally delivered into PL subregion (0.2 µl/hemisphere) or IL subregion (0.2 µl/hemisphere) of *Gabrd* KO mice. Four weeks after virus injections, the mice were subjected to behavioral training or *ex vivo* electrophysiological recording. All viruses were packaged by Obio Technology.

Statistics. The data analysis was performed with GraphPad Prism (GraphPad Software) or SPSS (IBM). The comparisons between two groups were assessed by a two-tailed unpaired *t* test (for normally distributed data) or Mann–Whitney *U* test (for non-normally distributed data). The correlation analysis was tested with Pearson's correlation test (for normally distributed data) or Spearman's correlation test (for non-normally distributed data). The more complicated datasets were analyzed with two-way ANOVA with or without repeated measures, followed by a *post hoc t* test with Bonferroni's correction (*p*-value of interaction, >0.05) or a simple-effect test with Bonferroni's correction (*p*-value of interaction, <0.05). The values over 3 SDs around the mean were excluded. The significance of statistics was considered at $p < 0.05$.

Results

ABA$_A$(δ)R expression and function in mPFC correlates with the extinction of learned fear in mice

To screen the GABA$_A$R subtypes that may signal fear extinction in mice, we subjected all the mice to a fear-conditioning and extinction procedure and divided them into Extinction-Success (ES) and Extinction-Failure (EF) groups based on their ability to recall extinction (Fig. 1*A*). Following fear conditioning, the tested mice displayed a robust increase in the conditioned fear response, which was markedly reversed by two subsequent sessions of extinction training (Fig. 1*B*; CS; Habituation: $F_{(2.853,51.35)} = 0.455$, $p = 0.706$; Fear learning: $F_{(3.273,58.92)} = 43.50$, $p < 0.001$; $F_{(2.399,43.18)} = 4.447$, $p = 0.013$; second Ext: $F_{(2.978,53.61)} = 7.135$, $p < 0.001$). Notably, the extent to which the mice extinguished the learned fear varied across individuals. We evaluated the Extinction-Retention Index (ERI) of the mice (Milad et al., 2008) and assigned them into the ES group with the top 40% ERI score or the EF group having the bottom 40% score (Fig. 1*C*; $t_{(18)} = 5.908$, $p < 0.001$). Although the two subgroups differed strikingly in terms of their retention of extinction memory, they showed similar fear responses to the cued tone over habituation, fear acquisition and within-session extinction (Fig. 1*B*; ERI; Habituation: $F_{(1,18)} = 0.626$, $p = 0.439$; Fear learning: $F_{(1,18)} = 0.775$, $p = 0.390$; first Ext: $F_{(1,18)} = 0.469$, $p = 0.502$; second Ext: $F_{(1,18)} < 0.001$, $p = 0.986$; Test: $F_{(1,18)} = 13.13$, $p = 0.002$). The extinction-learning index (ELI) was also comparable between ES and EF mice ($t_{(18)} = 0.374$, $p = 0.713$), indicating similar acquisition of extinction memory (Fig. 1*D*). This between-group difference occurring selectively in the retention of extinction memory but not in fear conditioning and extinction acquisition was similarly reported in rats with different extinction memory recall (Burgos-Robles et al., 2007; Peters et al., 2010) and in human beings with or without PTSD (Milad et al., 2008).

Next, we isolated the mPFC of ES and EF mice 24 h after the retention test and analyzed the transcriptional profiles of GABA$_A$R subunits, which are abundantly distributed in the forebrain (Hörtnagl et al., 2013). Somewhat surprisingly, among the diverse GABA$_A$R subunits, we observed that only the *Gabrd* mRNA level was significantly lower in EF mice relative to the ES ones (Fig. 1*E*; $t_{(18)} = 3.139$, $p = 0.006$). By contrast, the mRNA levels of other subunits were statistically indistinguishable between the two groups (*Gabra1*: $U = 34$, $p = 0.248$; *Gabra2*: $U = 48$, $p = 0.912$; *Gabra3*: $t_{(18)} = 0.793$, $p = 0.438$; *Gabra4*: $t_{(18)} = 0.227$, $p = 0.823$; *Gabra5*: $t_{(18)} = 0.876$, $p = 0.393$; *Gabrb1*: $t_{(18)} = 1.232$, $p = 0.234$; *Gabrb2*: $U = 42$, $p = 0.579$; *Gabrb3*: $t_{(18)} = 0.078$, $p = 0.939$; *Gabrg2*: $t_{(18)} = 0.897$, $p = 0.429$; *Gabrd*: $t_{(18)} = 3.139$, $p = 0.006$; *Gabrr1*: $t_{(18)} = 1.044$, $p = 0.310$). Further analysis revealed a significant and positive correlation between the *Gabrd* mRNA level and the ERI of the tested mice (Fig. 1*F*; $r = 0.584$, $p = 0.003$), suggesting that the *Gabrd* in mPFC may signal the ability of individual mice to extinguish the learned fear.

Since the *Gabrd* encodes the δ-subunit of GABA$_A$R that is preferentially situated in extrasynaptic membrane and mediates the tonic GABAergic inhibition in multiple cell types and brain regions (Whissell et al., 2015; Qin et al., 2022), we next explored whether the function of GABA$_A$(δ)R also differed between the mPFC of ES and EF mice (Fig. 1*G*,*K*). 2 µM THIP, which preferentially activates GABA$_A$(δ)R (Qin et al., 2022), was used to evoke GABA$_A$(δ)R-mediated tonic current in IL and PL cortices, two key mPFC subregions critical for fear regulation (Giustino and Maren, 2015). Comparisons of the current magnitude revealed that in IL cortex, the current was far stronger in ES mice (Fig. 1*H*,*I*; $t_{(8)} = 4.049$, $p = 0.004$), while in PL cortex, it was comparable between the two groups (Fig. 1*L*,*M*; $U = 6$, $p = 0.222$). Thus, it appears that the GABA$_A$(δ)R function is more prominent in the IL of ES mice relative to their EF counterparts. Moreover, the current strength in IL cortex ($r = -0.688$, $p = 0.014$), but not PL cortex ($r = -0.336$, $p = 0.286$), was positively correlated with the ERI (Fig. 1*J*,*N*). These findings well match with the established role of IL cortex in tuning fear extinction (Milad and Quirk, 2002). The phasic inhibition, which was known to be mediated by the synaptic GABA$_A$Rs, seems to be similar between the two groups in either mPFC subregion. Neither the frequency (IL cortex: $t_{(8)} = 0.007$, $p = 0.995$; PL cortex: $t_{(8)} = 0.319$, $p = 0.758$) nor the amplitude (IL cortex: $t_{(8)} = 581$, $p = 0.577$; PL cortex: $t_{(8)} = 1.795$, $p = 0.110$) of sIPSCs differed between the IL or PL subregion of the two mouse groups (Fig. 2). Altogether, the above findings imply that the GABA$_A$(δ)R in IL subregion may signal fear extinction in mice.

To clarify whether the different GABA$_A$(δ)R expression and function between ES and EF mice also occur in other brain regions enrolled in fear extinction, we repeated the above comparisons in the BLA (Fig. 3*A*). In sharp contrast to the mPFC, all the tested GABA$_A$R genes, including *Gabrd*, exhibited a comparable expression level between the two groups (Fig. 3*B*; *Gabra1*: $t_{(18)} = 0.532$, $p = 0.601$; *Gabra2*: $t_{(18)} = 1.193$, $p = 0.248$; *Gabra3*: $U = 48$, $p = 0.912$; *Gabra4*: $t_{(18)} = 1.604$, $p = 0.126$; *Gabra5*: $t_{(18)} = 1.625$, $p = 0.122$; *Gabrb1*: $t_{(18)} = 0.267$, $p = 0.792$; *Gabrb2*: $U = 34$, $p = 0.248$; *Gabrb3*: $t_{(18)} = 0.659$, $p = 0.518$; *Gabrg2*: $U = 43$, $p = 0.631$; *Gabrd*: $t_{(18)} = 0.692$, $p = 0.498$; *Gabrr1*: $t_{(18)} = 0.747$,

←

Comparisons of ELI in EF and ES mice. Same sample size as in ***B***. ***E***, Comparisons of the mRNA levels of GABA$_A$R subunits in the mPFC in ES and EF mice. Same sample size as in ***B***. ***F***, Correlations between the mRNA level of *Gabrd* in mPFC and the ERI of mice. ***G***, Schematic showing patch-clamp recording performed in the PNs of IL cortex. ***H***, Representative traces of THIP-evoked current of IL PNs from ES and EF mice. ***I***, Summary plots of the data in ***H***. ES, $n = 5$ mice; EF, $n = 5$ mice. ***J***, Correlations between the THIP-evoked current in IL PNs and the ERI of mice. Each data point for THIP-evoked current represent the average value of the data from three to five cells. ***K***, Schematic showing the patch-clamp recording performed in the PNs of PL cortex. ***L***, Representative traces of THIP-induced current of PL PNs from ES and EF mice. ***M***, Summary plots of the data in ***I***. ES, $n = 5$ mice; EF, $n = 5$ mice. ***N***, Correlations between the THIP-evoked current in PL PNs and the ERI of mice. Each data point for the THIP-evoked current represent the average value of the data from three to five cells. Data in ***G–N*** are from a separate group of mice. Data are presented as the mean ± SEM. $^*p < 0.05$, $^{**}p < 0.01$, $^{***}p < 0.001$.

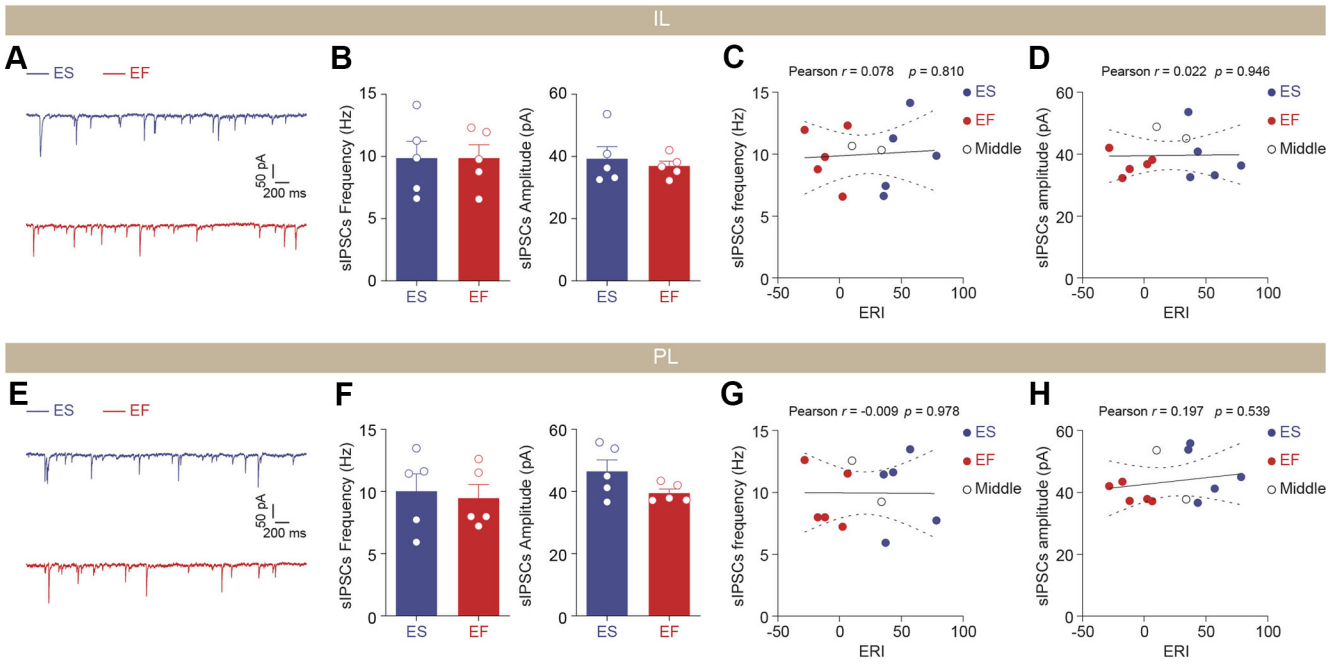

Figure 2. The phasic GABA$_A$R currents are similar in the mPFC PNs between ES and EF mice. ***A***, Representative traces showing sIPSCs of IL PNs from ES and EF mice. ***B***, Summary plots of the sIPSC frequency (left) and amplitude (right) in ***A***. ES, $n = 5$ mice; EF, $n = 5$ mice. ***C***, Correlation analysis of the IL sIPSC frequency with ERI of mice. ***D***, Correlation analysis of the IL sIPSC amplitude with ERI of mice. ***E***, Same as in ***A*** except that the data were from PL PNs. ***F***, Summary plots of the sIPSC frequency (left) and amplitude (right) in ***E***. ES, $n = 5$ mice; EF, $n = 5$ mice. ***G***, Correlation analysis of the PL sIPSC frequency with ERI of mice. ***H***, Correlation analysis of the PL sIPSC amplitude with ERI of mice. Data are presented as the mean ± SEM.

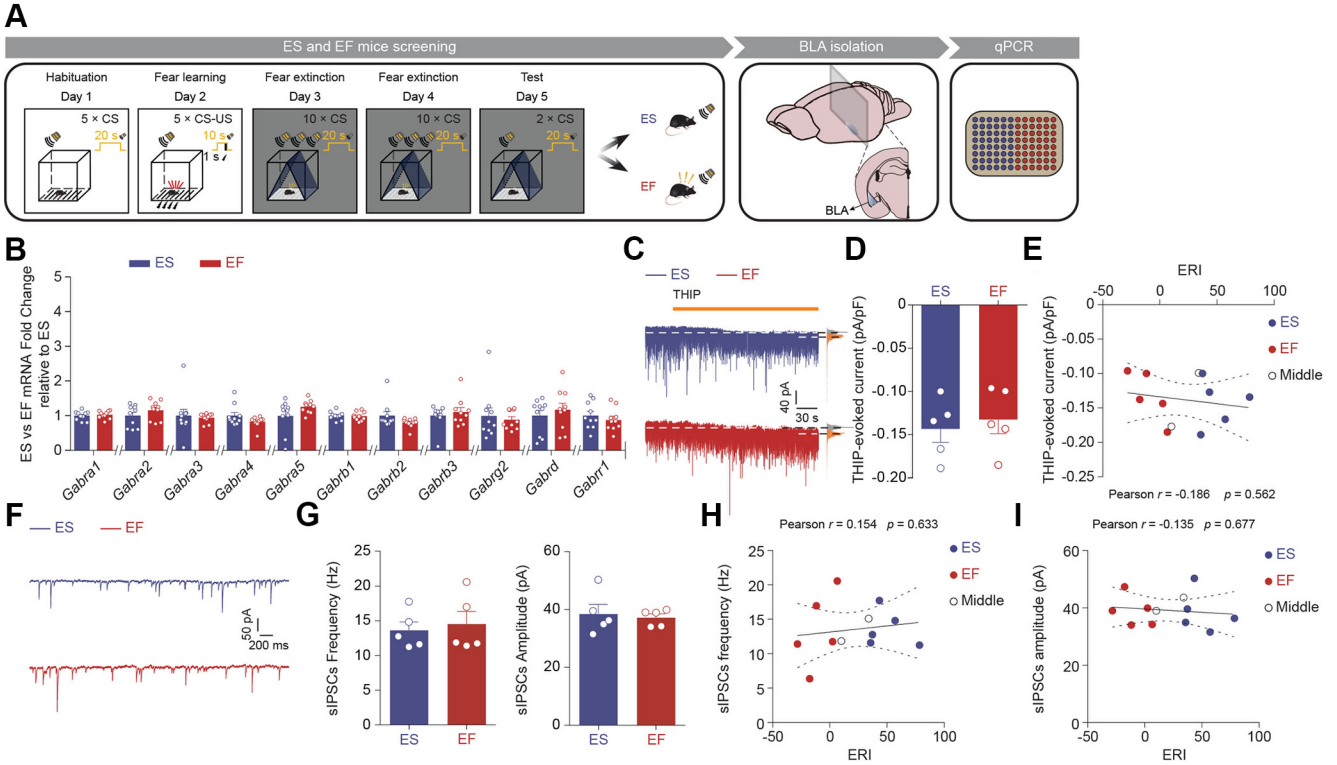

Figure 3. The mRNA levels of GABA$_A$R subunits, tonic and phasic GABA$_A$R currents are similar in the BLA between ES and EF mice. ***A***, Schematic illustration of fear conditioning and extinction paradigms for the screening of ES and EF mice, and subsequent BLA isolation and quantitative PCR tests. ***B***, Comparisons of the mRNA levels of GABA$_A$R subunits in the BLA between ES and EF mice. ES, $n = 10$ mice; EF, $n = 10$ mice. ***C***, Representative traces showing THIP-induced changes in the holding currents of BLA PNs from ES and EF mice. ***D***, Summary plots of the data in ***A***. ES, $n = 5$ mice; EF, $n = 5$ mice. ***E***, Correlation analysis of the THIP-induced changes in holding current in BLA PNs with ERI of mice. ***F***, Representative traces of sIPSCs of BLA PNs from ES and EF mice. ***G***, Summary plots of the sIPSC frequency (left) and amplitude (right) in ***F***. ES, $n = 5$ mice; EF, $n = 5$ mice. ***H***, Correlation analysis of the BLA sIPSC frequency with ERI of mice. ***I***, Correlation analysis of the BLA sIPSC amplitude with ERI of mice. Data are presented as the mean ± SEM.

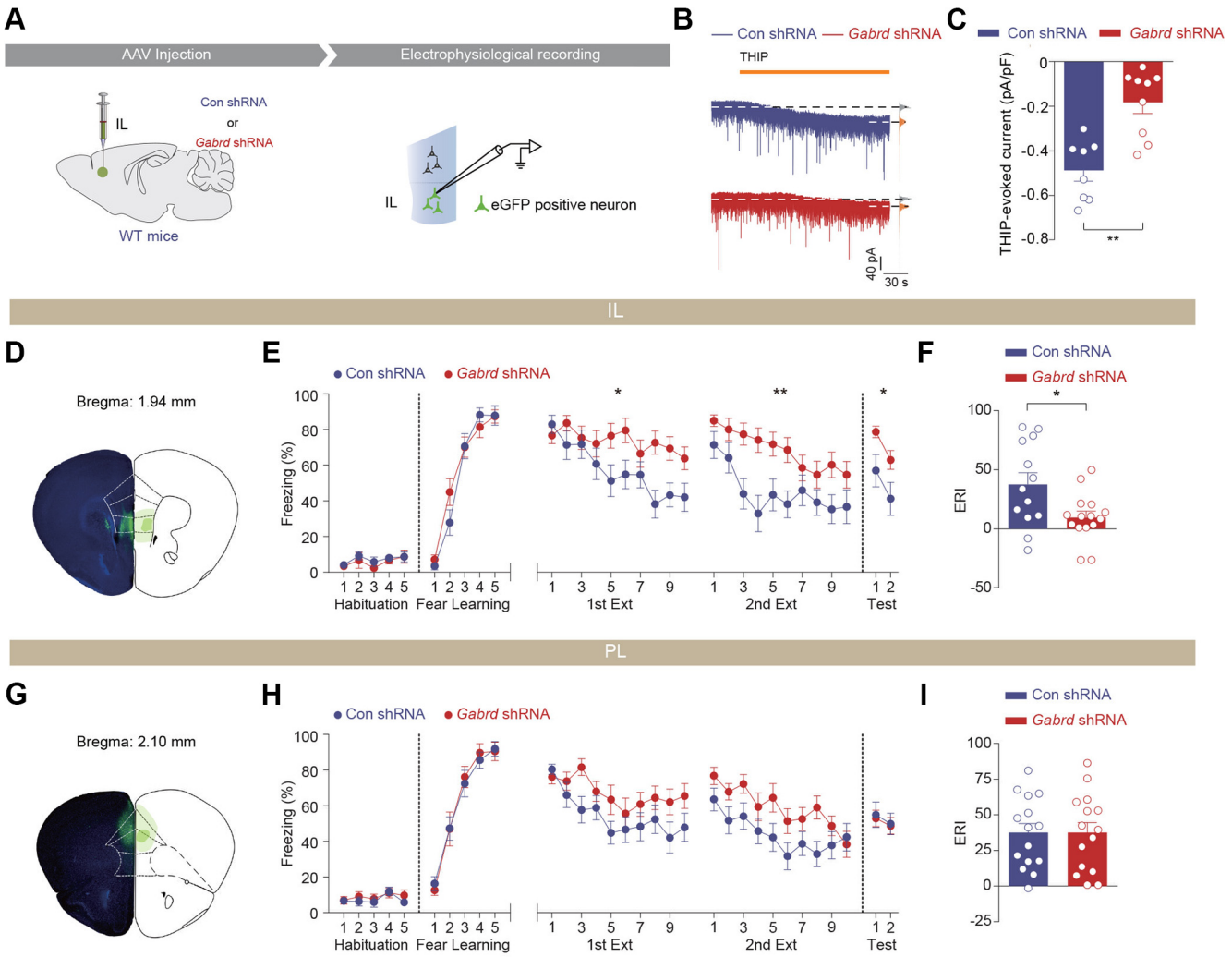

Figure 4. Impaired fear extinction by knocking down the GABA$_A$(δ)R expression in the IL of mice. ***A***, Schematic of AAV injection into the IL of mice to knock down *Gabrd* expression by shRNA (*Gabrd* shRNA) and subsequent patch-clamp recording. The empty shRNA vector (Con shRNA) was used as a control. ***B***, Representative traces of THIP-evoked current of IL PNs from Con shRNA and *Gabrd* shRNA groups of mice. ***C***, Summary plots of the data in ***B***. Con shRNA, $n = 8$ cells/3 mice; *Gabrd* shRNA, $n = 9$ cells/3 mice. ***D***, Representative images showing EGFP expression (green) in the IL subregion of an AAV-injected mouse, the minimum and maximum viral spread were denoted in dark green and light green. ***E***, The freezing levels of Con shRNA-injected or *Gabrd* shRNA-injected mice in response to CS during habituation, fear conditioning, extinction, and retrieval test. Con shRNA, $n = 13$; *Gabrd* shRNA, $n = 15$. ***F***, Comparisons of the ERI. Same sample size as in ***E***. ***G–I***, Same as in ***D–F*** except that the data were from mice that had received AAV injection in the PL. Con shRNA, $n = 15$; *Gabrd* shRNA, $n = 15$. Data are presented as the mean ± SEM. $^*p < 0.05$, $^{**}p < 0.01$.

$p = 0.465$). Consistently, the magnitudes of both tonic and phasic inhibitory currents (Fig. 3*C*,*D*: tonic current: $t_{(8)} = 0.482$, $p = 0.643$; Fig. 3*F*,*G*: sIPSC frequency: $t_{(8)} = 0.404$, $p = 0.697$; sIPSC amplitude: $t_{(8)} = 0.379$, $p = 0.715$) did not differ between the two groups, and showed no correlation with the ERI of the mouse (Fig. 3*E*: tonic current: $r = -0.186$, $p = 0.562$; Fig. 3*H*: sIPSC frequency: $r = 0.154$, $p = 0.633$; Fig. 3*G*: sIPSC amplitude: $r = -0.135$, $p = 0.677$).

Knockdown of GABA$_A$(δ)R in IL but not PL impairs fear extinction

Fear extinction is regarded as a form of inhibitory learning that suppresses fear expression (Pape and Pare, 2010; Singewald et al., 2015). The GABA$_A$Rs in mPFC were also shown to suppress the extinction of learned fear (Sierra-Mercado et al., 2011; Marek et al., 2018a; Chen et al., 2022). We reasoned that if the GABA$_A$(δ)R in IL subregion coordinates with other GABA$_A$R subtypes to inhibit the activity of mPFC neurons, it would similarly suppress fear extinction as other GABA$_A$Rs do (Sierra-Mercado et al., 2011). However, the positive correlations of the *Gabrd* mRNA expression and the GABA$_A$(δ)R-mediated tonic current with the ERI in individual mice indicate that GABA$_A$(δ)R in IL subregion facilitates but does not suppress fear extinction. A critical question thus arises regarding the exact role of GABA$_A$(δ)R in IL subregion in regulating fear extinction.

To answer this question, we first investigated the effect of downregulating GABA$_A$(δ)R function in IL on fear extinction in mice. The short hairpin RNA (shRNA) vector targeting *Gabrd* mRNA (*Gabrd* shRNA) with an enhanced green fluorescent protein (EGFP) reporter was constructed and packaged into adeno-associated viruses (AAVs), whereas the empty vector was used as the control (Con shRNA; Fig. 4*A*). AAVs were injected into the IL or PL subregion of WT mice, respectively. The effectiveness of *Gabrd* shRNA in downregulating GABA$_A$(δ)R function was confirmed by the significant reduction of tonic inhibition in IL pyramidal neurons (PNs) after injection (Fig. 4*B*,*C*; $U = 6$, $p = 0.003$). We then submitted the mice to fear conditioning and extinction (Fig. 4*D–F*). While the Con shRNA-injected and *Gabrd* shRNA-injected mice showed similar freezing during

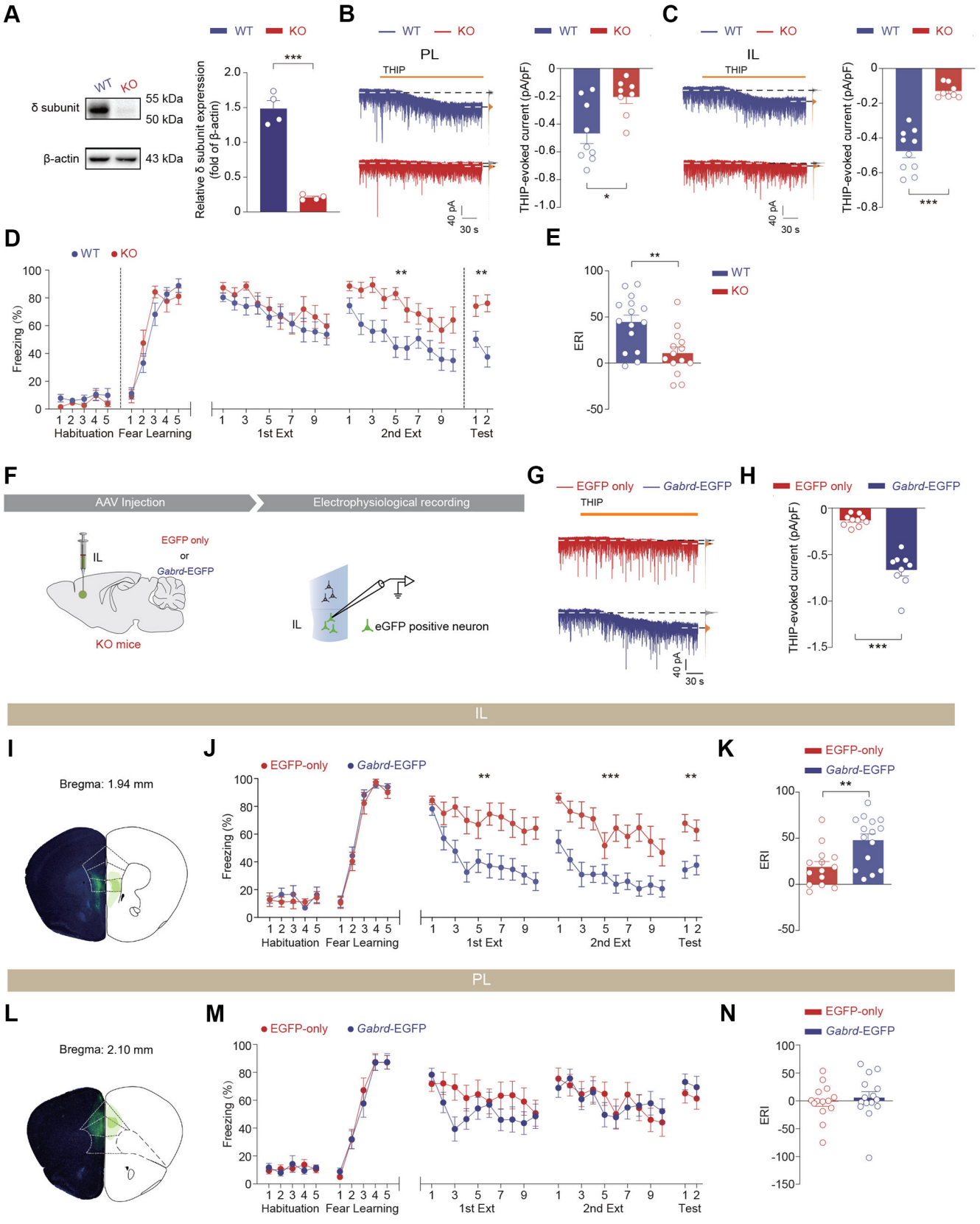

Figure 5. Rescue of fear extinction deficit in the *Gabrd* KO mice by re-expressing GABA$_A$(δ)R in IL. ***A***, Left, Representative immunoblot of δ-subunit in mPFC collected from the WT and KO mice. Right, Quantification analysis of relative δ-subunit expression (band intensity of δ-subunit/β-actin), WT mice, $n = 4$; KO mice, $n = 4$. ***B***, Left, Representative traces showing a THIP-evoked current obtained from the PL PNs of WT and KO mice. Right, Summary plots of data in left panel. WT, $n = 9$ cells/3 mice; KO, $n = 8$ cells/3 mice. ***C***, Same as in ***B*** except that the data were from IL PNs. WT, $n = 10$ cells/3 mice; KO, $n = 8$ cells/3 mice. ***D***, The freezing levels of WT and KO mice in response to CS during habituation, fear conditioning, extinction, and retrieval test. WT, $n = 15$; KO, $n = 14$. ***E***, Comparisons of ERI. Same sample size as in ***D***. ***F***, Schematic of AAV injection to overexpress GABA$_A$(δ)R (*Gabrd*-EGFP) or EGFP alone (EGFP-only) under *synapsin I* (SYN) promoter in the IL of KO mice and subsequent patch-clamp recording. ***G***, Representative traces showing THIP-evoked current of IL PNs of EGFP-only-injected or *Gabrd*-EGFP-injected KO

habituation and fear conditioning, the latter had higher freezing during the extinction training and test sessions (Fig. 4*E*; *Gabrd* knockdown; Habituation: $F_{(1,26)} = 0.548$, $p = 0.466$; Fear learning: $F_{(1,26)} = 0.388$, $p = 0.539$; first Ext: $F_{(1,26)} = 5.262$, $p = 0.030$; second Ext: $F_{(1,26)} = 8.102$, $p = 0.009$; Test: $F_{(1,26)} = 5.644$, $p = 0.025$), leading to a lower ERI (Fig. 4*F*; $t_{26} = 2.592$, $p = 0.016$). In line with the absence of correlation between the $GABA_A(\delta)$R expression or function in PL subregion and the ERI (Fig. 1*N*), knocking down the $GABA_A(\delta)$R expression in PL neurons failed to affect fear extinction (Fig. 4*H*: *Gabrd* knockdown; Habituation: $F_{(1,28)} = 0.531$, $p = 0.472$; Fear learning: $F_{(1,28)} = 0.016$, $p = 0.901$; first Ext: $F_{(1,28)} = 2.838$, $p = 0.103$; second Ext: $F_{(1,28)} = 3.803$, $p = 0.061$; Test: $F_{(1,28)} = 1.454$, $p = 0.238$; Fig. 4*I*: ERI: $t_{(28)} = 0.009$, $p = 0.993$). Thus, these data also suggest a permissive role of $GABA_A(\delta)$R in IL subregion for fear extinction.

Re-expression of $GABA_A(\delta)$R in the IL of *Gabrd* KO mice suffices to reverse the deficits of fear extinction

We further tested the role of $GABA_A(\delta)$R in mPFC for fear extinction by using the *Gabrd* knock-out (KO) mice. Western blotting result with anti-$GABA_A(\delta)$R antibody demonstrated a significant ablation of *Gabrd* expression in the mPFC of KO mice (Fig. 5*A*; $t_{(6)} = 11.03$, $p < 0.001$). The recording of $GABA_A(\delta)$R-mediated tonic currents also yielded $GABA_A(\delta)$R loss of function in both IL ($t_{(16)} = 2.932$, $p = 0.010$) and PL ($t_{(15)} = 7.690$, $p < 0.001$) subregions of KO mice (Fig. 5*B*,*C*). The effects of $GABA_A(\delta)$R deficiency on fear extinction was then investigated. Either KO mice or their WT littermates showed similar freezing responses during habituation, fear learning, and even the first session of extinction training (Fig. 5*D*; Genotype; Habituation: $F_{(1,27)} = 2.371$, $p = 0.135$; Fear learning: $F_{(1,27)} = 0.328$, $p = 0.572$; first Ext: $F_{(1,27)} = 0.790$, $p = 0.382$). However, the KO mice displayed more robust freezing during the second session of extinction training and on the retention of extinction memory on day 5 (Fig. 5*D*; Genotype; second Ext: $F_{(1,27)} = 9.922$, $p = 0.004$; Test: $F_{(1,27)} = 12.40$, $p = 0.002$), resulting in a weaker ERI (Fig. 5*E*; $t_{(27)} = 3.379$, $p = 0.002$). These results demonstrated that $GABA_A(\delta)$R deficiency leads to impairment of fear extinction with little influence on fear conditioning.

To test the necessity of $GABA_A(\delta)$R in the IL for fear extinction, we reintroduced the δ-subunit into the IL neurons of KO mice through AAVs. AAV-SYN-*Gabrd*-2A-EGFP (*Gabrd*-EGFP) or AAV-SYN-EGFP (EGFP-only) were injected into the IL subregion of KO mice (Fig. 5*F*). As shown in Figure 5, *G* and *H*, the THIP-evoked currents in the IL PNs from *Gabrd*-EGFP mice were far stronger than those from the EGFP-only mice ($t_{(17)} = 3.379$, $p = 0.002$), substantiating the effectiveness of $GABA_A(\delta)$R re-expression in producing the tonic inhibition in IL PNs.

We next investigated whether reintroducing $GABA_A(\delta)$R in the IL subregion of KO mice could reverse the impaired fear extinction. As shown in Figure 5*I*–*K*, although both groups displayed comparable levels of freezing during habituation and fear conditioning, the *Gabrd*-EGFP group showed substantially weaker freezing during the first and second session of extinction training as well as the retention test (*Gabrd* overexpression; Habituation: $F_{(1,27)} = 0.192$, $p = 0.665$; Fear learning: $F_{(1,27)} = 0.363$, $p = 0.552$; first Ext: $F_{(1,27)} = 10.96$, $p = 0.003$; second Ext: $F_{(1,27)} = 16.79$, $p < 0.001$; Test: $F_{(1,27)} = 11.98$, $p = 0.002$), with a higher ERI score ($t_{(27)} = 3.209$, $p = 0.003$). *Gabrd* re-expression in the PL subregion of KO mice, however, had little effect on the freezing responses throughout the behavioral training and test (Fig. 5*M*: *Gabrd* overexpression; Habituation: $F_{(1,27)} < 0.001$, $p = 0.978$; Fear learning: $F_{(1,27)} = 0.033$, $p = 0.858$; first Ext: $F_{(1,27)} = 1.340$, $p = 0.257$; second Ext: $F_{(1,27)} = 0.017$, $p = 0.896$; Test: $F_{(1,27)} = 0.791$, $p = 0.382$; Fig. 5*N*: ERI: $U = 93$, $p = 0.621$).

Combined together, the above findings strongly suggest that the $GABA_A(\delta)$R in IL subregion promotes the extinction of learned fear. Since both $GABA_A(\delta)$R and other $GABA_A$R members contribute to the inhibitory signals in mPFC, how could $GABA_A(\delta)$R affect fear extinction in an opposite way to the $GABA_A$R family? Are there any unique mechanisms for $GABA_A(\delta)$R to have its permissive role in fear extinction? In the following experiments, we attempted to answer these questions by using the *Gabrd* KO mice and their WT littermates.

$GABA_A(\delta)$R deficiency occludes IL neuronal activation on fear extinction

We first examined the effects of $GABA_A(\delta)$R on IL activity during fear extinction through immunostaining the c-*Fos*, an immediate early gene indicator for activated neurons (Flavell and Greenberg, 2008). Either KO or WT mice were randomly assigned to three experimental groups as shown in Figure 6*A* (also see Materials and Methods). One hour and 30 min after the delivery of the last CS on day 5, the mice brains were collected for c-*Fos* staining (Fig. 6*A*). Two-way ANOVA revealed a significant main effect on the interaction between genotype and behavioral training for the c-*Fos* expression (Interaction: $F_{(2,24)} = 3.558$, $p = 0.044$). *Post hoc* simple-effect tests showed the following: (1) the number of c-Fos^+ cells in KO mice was far more than that in the WT mice ($p = 0.020$; Fig. 6*B*,*C*), suggesting that $GABA_A(\delta)$R deficiency per se markedly increased the neuronal activity in IL subregion; (2) for the WT mice, the number of c-Fos^+ cells was significantly higher in the Ext group than the CS Only and No Ext groups (CS Only vs No Ext, $p > 0.999$; CS Only vs Ext, $p = 0.015$; No Ext vs Ext, $p = 0.003$); and (3) for the KO mice, the number of c-Fos^+ cells was similar among the three groups (CS Only vs No Ext, $p > 0.999$; CS Only vs Ext, $p > 0.999$; No Ext vs Ext, $p > 0.999$; Fig. 6*B*,*C*). Thus, it appears that fear extinction leads to increased activation of IL neurons, which could be occluded by $GABA_A(\delta)$R deficiency.

$GABA_A(\delta)$R deficiency does not affect the plasticity of glutamatergic transmission in IL neurons during extinction

The increased neuronal activity in IL on extinction may result from the adaptative changes of IL neurons per se and/or their cross talk with other interconnected cells. Multiple lines of evidence have shown that the plasticity of GABAergic and glutamatergic transmission onto IL neurons are key participants in the altered IL activity by fear extinction (Pattwell et al., 2012; Wang et al., 2018). Given the essential role of $GABA_A(\delta)$R in regulating synaptic plasticity and memory (Whissell et al., 2013a; Liu et al., 2017), we asked whether the diminished change of neuronal activity following *Gabrd* KO was a consequence of altered plasticity of synaptic transmission. We assigned the WT and KO mice to the experimental groups, as shown in Figure 6*A*.

←

mice. ***H***, Summary plot of data in ***G***. EGFP-only, 10 cells/3 mice; *Gabrd*-EGFP, 9 cells/3 mice. ***I***, Representative images showing EGFP expression in IL subregion, the minimum and maximum viral spread were denoted in dark green and light green. ***J***, The freezing levels of EGFP-only-injected or *Gabrd*-EGFP-injected KO mice in response to CS during habituation, fear conditioning, extinction, and retrieval test. EGFP-only, $n = 14$; *Gabrd*-EGFP, $n = 15$. ***K***, Comparisons of ERI. Same sample size as in ***J***. ***L–N***, Same as in ***I–K*** except that the data were from mice received AAV injection in PL. EGFP-only, $n = 14$; *Gabrd*-EGFP, $n = 15$. Data are presented as the mean ± SEM. $^*p < 0.05$, $^{**}p < 0.01$, $^{***}p < 0.001$.

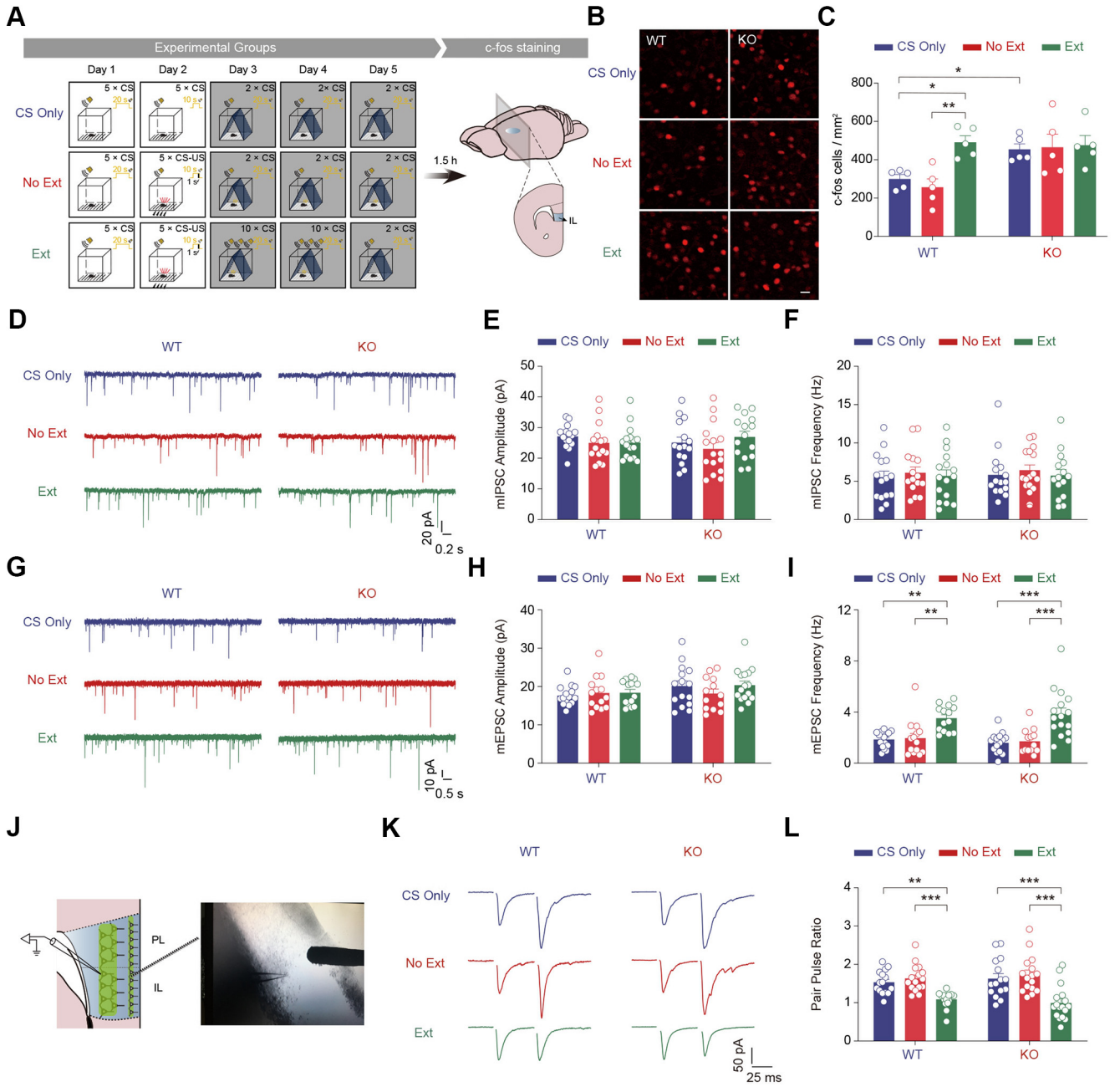

Figure 6. *Gabrd* knockout does not alter extinction-evoked changes in synaptic transmission. ***A***, Schematics of behavioral training paradigms and subsequent c-*Fos* immunostaining. ***B***, Representative images of c-*Fos* expression in the IL subregions of both genotypes in CS Only, No Ext, and Ext groups. Scale bar, 20 μm. ***C***, Summary plots of data in ***B***. For WT: CS Only, $n = 5$ mice; No Ext, 5 mice; Ext, 5 mice. For KO: CS Only, $n = 5$ mice; No Ext, 5 mice; Ext, 5 mice. ***D***, Representative traces showing mIPSCs recorded from the IL PNs of WT and KO mice in CS Only, No Ext, and Ext groups. ***E***, Summary of the mIPSC amplitude in ***A***. WT: CS Only, $n = 15$ cells/5 mice; No Ext, 15 cells/5 mice; Ext, 16 cells/5 mice; KO: CS Only, $n = 15$ cells/5 mice; No Ext, 16 cells/5 mice; Ext, 15 cells/5 mice. ***F***, Summary of the mIPSC frequency in ***D***. Same sample size as in ***E***. ***G***, Representative traces of mEPSCs recorded from the IL PNs of WT and KO mice in CS Only, No Ext, and Ext groups. ***H***, Summary plots of the mEPSC amplitude in ***G***. WT: CS Only, $n = 15$ cells/5 mice; No Ext, 14 cells/5 mice; Ext, $n = 14$ cells/5 mice; KO: CS Only, $n = 15$ cells/5 mice; No Ext, 13 cells/4 mice; Ext, 16 cells/5 mice. ***I***, Summary plots of the mEPSC frequency in ***H***. Same sample size as in ***H***. ***J***, Left, Schematic showing the placement of stimulation electrode in layer II/III and the patch-clamp recording in layer V PNs in IL subregion. Right, Corresponding images showing the positions of stimulation and recording electrodes in IL subregion. ***K***, Representative traces of evoked EPSCs in IL PNs on paired stimuli with an interval of 50 ms. ***L***, Summary plots of PPR in ***H***. WT: CS Only, $n = 15$ cells/5 mice; No Ext, 16 cells/5 mice; Ext, 15 cells/5 mice; KO: CS Only, $n = 15$ cells/5 mice; No Ext, 16 cells/5 mice; Ext, 17 cells/5 mice. Data are presented as the mean ± SEM. *$p < 0.05$, **$p < 0.01$, ***$p < 0.001$.

The electrophysiological recordings were performed in the layer V PNs of IL, which have extensive connections with multiple subcortical regions engaged in fear expression and regulation (Adhikari et al., 2015; Giustino and Maren, 2015). We first examined the GABAergic and glutamatergic neurotransmission by measuring the mIPSCs and mEPSCs in IL neurons. The amplitudes (Genotype: $F_{(1,86)} = 0.261$, $p = 0.611$; Behavioral training; $F_{(2,86)} = 1.012$, $p = 0.368$; Interaction; $F_{(2,86)} = 0.957$, $p = 0.388$) and frequencies (Genotype; $F_{(1,86)} = 0.139$, $p = 0.711$; Behavioral training; $F_{(2,86)} = 0.369$, $p = 0.693$; Interaction; $F_{(2,86)} = 0.024$, $p = 0.976$) of the mIPSCs were indistinguishable across different behavioral paradigms between the two genotypes (Fig. 6*D–F*). For the mEPSCs in both genotypes, their frequencies were increased by nearly twice in the Ext group relative to that in the CS Only or No Ext group (Behavioral training: $F_{(2,81)} = 24.50$, $p < 0.001$, *post hoc t* test; WT mice: CS Only vs

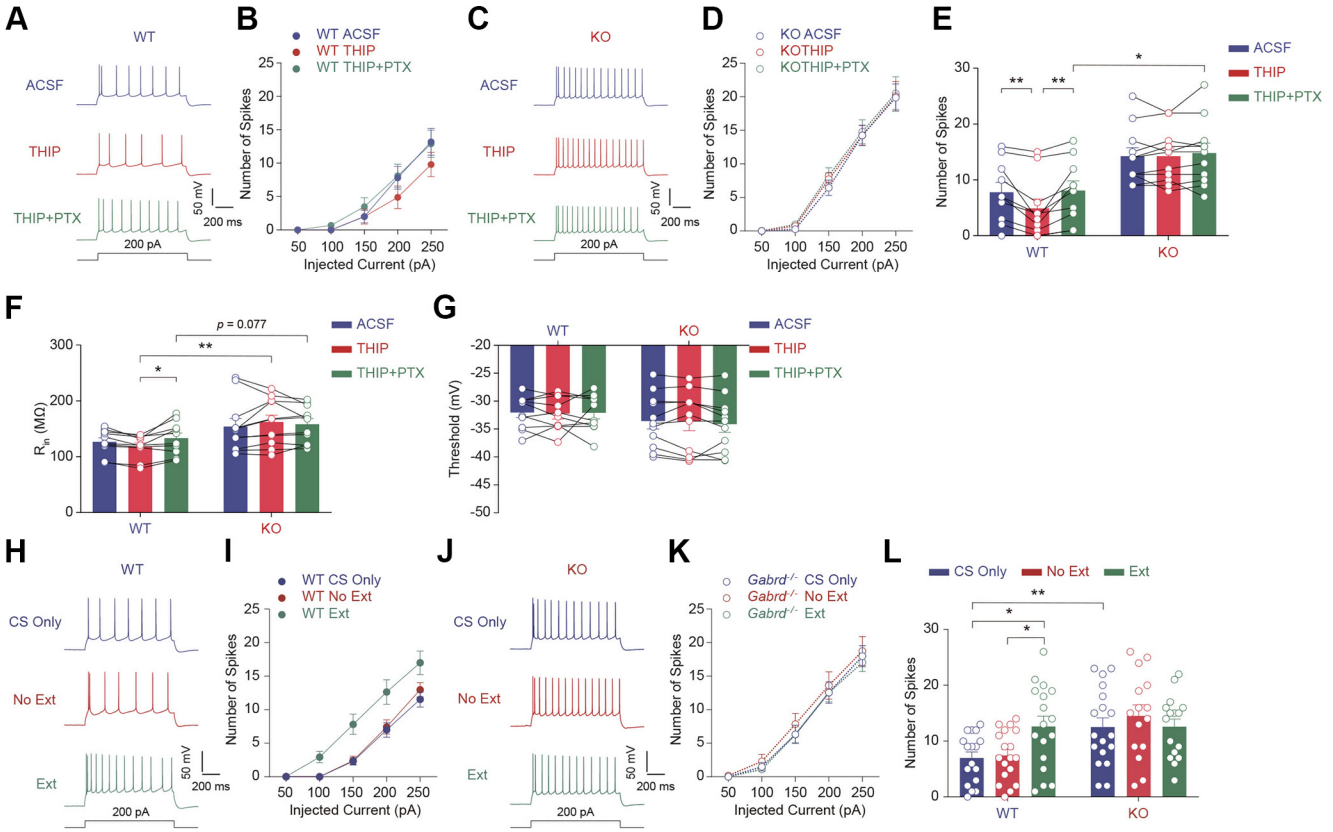

Figure 7. *Gabrd* knockout deprives the extinction-evoked changes in the excitability of IL PNs. ***A***, Representative traces showing the firing of IL PNs from WT mice in response to 200 pA depolarizing current injection when the slice is successively perfused with ACSF, THIP, and THIP + PTX. ***B***, Summary plots of action potential numbers induced by different depolarizing current injection in ***A***; WT: $n = 10$ cells/4 mice. ***C***, ***D***, Same as in ***A*** and ***B*** except that the data from KO mice. $n = 11$ cells/5 mice. ***E***, Quantitative analysis of action potential numbers of IL PNs at the 200 pA injected current from WT or KO mice on the treatment of ACSF, THIP, or THIP + PTX. Same sample size as in ***B*** and ***D***. ***F***, The R_{in} of IL PNs from WT and KO mice in the treatment with ACSF, THIP, or THIP + PTX. Same sample size as in ***B*** and ***D***. ***G***, The firing threshold of IL PNs from WT and KO mice in the treatment of ACSF, THIP, or THIP + PTX. Same sample size as in ***B*** and ***D***. ***H***, Representative traces showing the neuronal firing of IL PNs from WT mice in response to current injections (200 pA, 1 s). ***I***, Summary plots of the number of action potentials induced by different depolarizing current injections in ***H***. CS Only, $n = 17$ cells/5 mice; No Ext, 18 cells/5 mice; Ext, 17 cells/5 mice. ***J***, ***K***, Same as in ***H*** and ***I*** except that the data were from KO mice. CS Only, $n = 18$ cells/5 mice; No Ext, $n = 15$ cells/5 mice; Ext, $n = 16$ cells/5 mice. ***L***, Quantitative analysis of action potential numbers of IL PNs at 200 pA injected current from WT or KO mice in the CS Only, No Ext, and Ext groups. Same sample sizes as in ***I*** and ***K***. Data are presented as the mean ± SEM. *$p < 0.05$, **$p < 0.01$.

No Ext, $p > 0.999$; CS Only vs Ext, $p = 0.001$; No Ext vs Ext, $p = 0.003$; KO mice: CS Only vs No Ext, $p > 0.999$; CS Only vs Ext, $p < 0.001$; No Ext vs Ext, $p < 0.001$), with a similar amplitude among three groups (Genotype: $F_{(1,81)} = 2.580$, $p = 0.112$; Behavioral training: $F_{(2,81)} = 0.541$, $p = 0.585$; Interaction: $F_{(2,81)} = 0.809$, $p = 0.449$; Fig. 6*G–I*). Thus, it seems that fear extinction selectively augments the glutamatergic transmission into IL neurons, and *Gabrd* KO has little influence on glutamatergic transmission under resting state and its plasticity on fear extinction.

To further confirm these, we performed an additional experiment in which we delivered two stimuli to the inputs from layer II/III of IL and recorded the evoked EPSCs in layer V neurons (Fig. 6*J*; also see Materials and Methods). We observed that the PPR, which is known to correspond with the presynaptic release of glutamate transmitter, was significantly weaker in their Ext group relative to the other two groups, supporting enhanced glutamatergic transmission from layer II/III to layer V neurons by extinction training (Fig. 6*K*,*L*; Behavioral training: $F_{(2,88)} = 24.18$, $p < 0.001$, *post hoc t* test; WT mice: CS Only vs No Ext, $p = 0.843$; CS Only vs Ext, $p = 0.008$; No Ext vs Ext, $p < 0.001$; KO mice: CS Only vs No Ext, $p = 0.843$; CS Only vs Ext, $p < 0.001$; No Ext vs Ext, $p < 0.001$). However, no difference was found between genotypes, further arguing against the role of GABA$_A$(δ)R in tuning the extinction-evoked plasticity of glutamatergic transmission in IL neurons.

GABA$_A$(δ)R enables the plastic changes of neuronal excitability during fear extinction

In addition to eliciting plasticity of synaptic transmission in IL subregion, fear extinction was also found to alter the activity of IL neurons by modulating their intrinsic excitability (Santini et al., 2008; Bloodgood et al., 2018). GABA$_A$(δ)R has been repetitively shown to limit neuronal firing across numerous brain regions (Liu et al., 2017; Qin et al., 2022), raising the possibility that GABA$_A$(δ)R may regulate the extinction-evoked dynamics of neuronal activity in IL subregion through influencing their excitability.

We then switched to examine the potential impacts of GABA$_A$(δ)R on the excitability of IL neurons. For this, we injected the depolarizing current pulses with different intensities into the IL neurons to evoke firing, followed by perfusion with the GABA$_A$(δ)R agonist THIP only or plus the GABA$_A$R antagonist PTX. As shown in Figure 7*A–D*, the firing frequency was gradually increased in neurons of both genotypes with the increasing intensity of the injected current (Current injection; WT mice: $F_{(1.290,11.61)} = 30.28$, $p < 0.001$; KO mice: $F_{(1.084,10.84)} = 77.85$, $p < 0.001$). Notably, THIP markedly

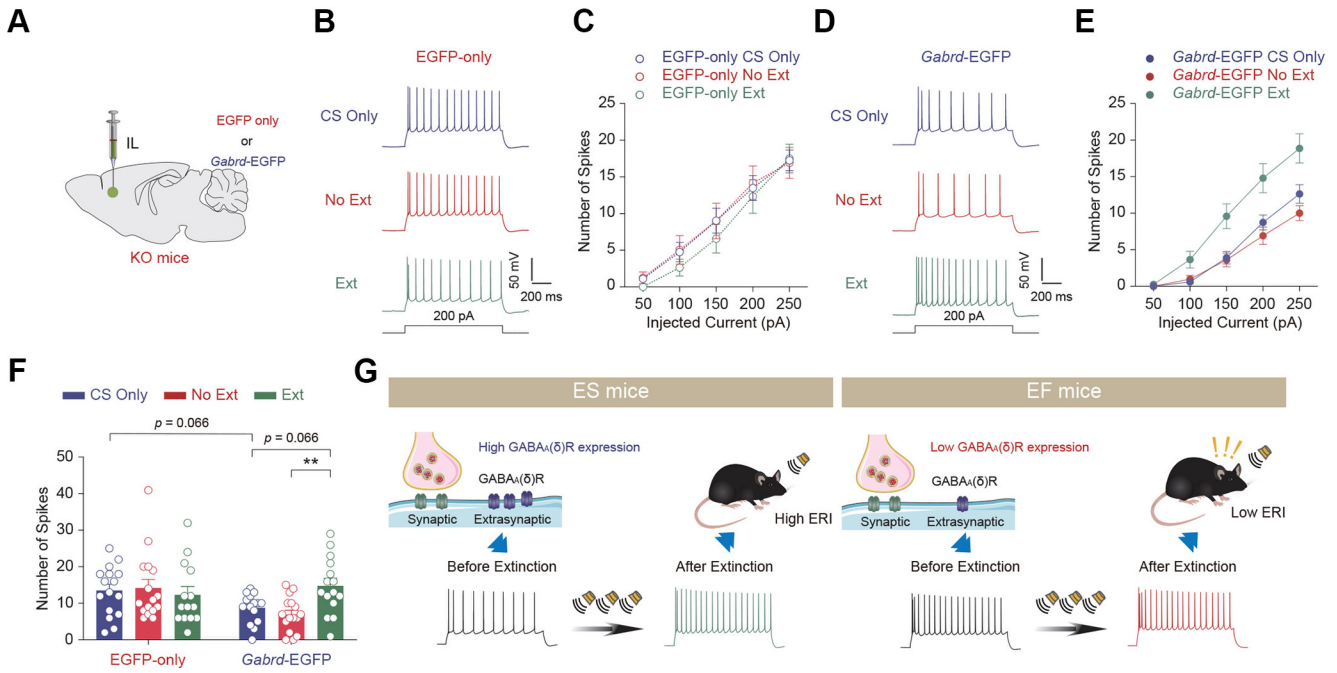

Figure 8. Re-expressing *Gabrd* in the IL of KO mice reverses the defective plastic change of neuronal excitability by fear extinction. ***A***, Schematic of AAV injection to express GABA$_A$(δ)R (*Gabrd*-EGFP) or EGFP alone (EGFP-only) under *synapsin I* (SYN) promoter in the IL subregion of KO mice. ***B***, Representative traces showing neuronal firing of IL PNs from EGFP-only mice after indicated behavioral training, in response to current injections (200 pA, 1 s). ***C***, Summary plots of the number of action potentials induced by different depolarizing current injections. CS Only, $n = 16$ cells/5 mice; No Ext, 16 cells/5 mice; Ext, 14 cells/5 mice. ***D***, ***E***, Same as in ***B*** and ***C*** except that the data were from *Gabrd*-EGFP mice. CS Only, $n = 15$ cells/5 mice; No Ext, 16 cells/5 mice; Ext, 15 cells/5 mice. ***F***, Quantitative analysis of the action potential numbers in the IL PNs from EGFP-only and *Gabrd*-EGFP mice in the CS Only, No Ext, and Ext groups. The 200 pA depolarization currents were delivered. Same sample size as in ***C*** and ***E***. ***G***, A working model for the role of *Gabrd* in IL in facilitating fear extinction. Data are presented as the mean ± SEM. $^{**}p < 0.01$.

suppressed the neuronal firing of the IL PNs from WT mice but not KO mice, and this effect was reversed by subsequent application of PTX (Fig. 7*A*,*B*: Pharmacological treatment; WT mice: $F_{(1.825,16.43)} = 17.93$, $p < 0.001$; Fig. 7*C*,*D*: Pharmacological treatment; KO mice; $F_{(1.631,16.31)} = 1.771$, $p = 0.204$; Fig. 7*E*: Pharmacological treatment: $F_{(1.953,37.11)} = 8.055$, $p = 0.001$; Genotype: $F_{(1,19)} = 11.01$, $p = 0.004$; Interaction: $F_{(2,38)} = 5.399$, $p = 0.009$; *post hoc* simple-effect tests; WT mice: ACSF vs THIP, $p = 0.002$; ACSF vs THIP + PTX, $p > 0.999$; THIP vs THIP + PTX, $p = 0.001$; KO mice: CS Only vs No Ext, $p > 0.999$; CS Only vs Ext, $p > 0.999$; No Ext vs Ext, $p = 0.999$), indicating a suppressive role of GABA$_A$(δ)R in regulating the excitability of IL PNs. The suppression of neuronal firing by GABA$_A$(δ)R may relate to its ability to regulate the input resistance (R_{in}) of IL neurons because the R_{in} was conspicuously increased following *Gabrd* KO with the firing threshold being intact (Fig. 7*F*: R_{in}: Pharmacological treatment: $F_{(1.723,32.74)} = 1.365$, $p = 0.267$; Genotype: $F_{(1,19)} = 5.251$, $p = 0.034$; Interaction: $F_{(2,38)} = 3.506$, $p = 0.040$; *post hoc* simple-effect tests, WT mice: ACSF vs THIP, $p = 0.324$; ACSF vs THIP + PTX, $p > 0.999$; THIP vs THIP + PTX, $p = 0.017$; KO mice: CS Only vs No Ext, $p = 0.405$; CS Only vs Ext, $p > 0.999$; No Ext vs Ext, $p = 0.999$; Fig. 7*G*: Firing threshold; Pharmacological treatment: $F_{(1.744,33.14)} = 0.242$, $p = 0.757$; Genotype: $F_{(1,19)} = 0.847$, $p = 0.369$; Interaction: $F_{(2,38)} = 0.268$, $p = 0.766$).

We next sought to explore whether the GABA$_A$(δ)R participated in the dynamics of IL PN excitability on fear learning and extinction. GABA (5 μM) was routinely added into the perfusion solution to ensure the activation of GABA$_A$(δ)R. At basal condition (CS Only group), the firing number of IL PNs was sharply higher in KO mice (Fig. 7*H*,*J*,*L*; Genotype: $F_{(1,95)} = 11.69$, $p < 0.001$; Behavioral training: $F_{(2,95)} = 1.807$, $p = 0.170$; Interaction: $F_{(2,95)} = 3.126$, $p = 0.048$; *post hoc* simple-effect test; WT vs KO mice: CS Only, $p = 0.010$). While fear conditioning had no effect on the firing number in both genotypes, fear extinction robustly enhanced the firing number in WT mice but not KO mice (Fig. 7*H–L*; *post hoc* simple-effect tests; WT mice: CS Only vs No Ext, $p > 0.999$; CS Only vs Ext, $p = 0.030$; No Ext vs Ext, $p = 0.048$; KO mice: CS Only vs No Ext, $p > 0.999$; CS Only vs Ext, $p > 0.999$; No Ext vs Ext, $p > 0.999$). Together with the extinction-evoked alteration of c-*Fos* expression, these results led us to speculate that the GABA$_A$(δ)R act to enable the extinction-evoked plastic regulation of neuronal excitability in IL subregion.

GABA$_A$(δ)R re-expression in the IL subregion of *Gabrd* KO mice rescues the defective dynamics of neuronal excitability on fear extinction

Finally, we asked whether the re-expression of the δ-subunit in IL subregion reverses the loss of plasticity of neuronal excitability by *Gabrd* KO mice, as it did on the fear extinction deficit (Fig. 8*A*). In mice expressing EGFP-only, both fear conditioning and extinction failed to alter the spike number of the PNs (Fig. 8*B*,*C*,*F*; *Gabrd* overexpression: $F_{(1,86)} = 4.603$, $p = 0.035$; Behavioral training: $F_{(2,86)} = 1.518$, $p = 0.225$; Interaction: $F_{(2,86)} = 3.745$, $p = 0.022$; *post hoc* simple-effect tests; EGFP-only: CS Only vs No Ext, $p > 0.999$; CS Only vs Ext, $p > 0.999$; No Ext vs Ext, $p > 0.999$). However, in mice expressing the GABA$_A$(δ)R (*Gabrd*-EGFP), the extinction training did increase the firing of IL neurons, indicating that reintroduction of GABA$_A$(δ)R was sufficient to reverse the loss of the plastic changes of excitability by *Gabrd* KO (Fig. 8*D–F*; *post hoc* simple-effect tests; *Gabrd*-EGFP: CS Only vs No Ext, $p > 0.999$; CS Only vs Ext, $p = 0.009$; No Ext vs Ext, $p = 0.066$). Therefore, the GABA$_A$(δ)R in IL subregion enables the dynamics of neuronal excitability during extinction, which is essential for the successful extinction of fear memory.

Discussion

In this study, we report that the $GABA_A(\delta)R$ in the IL subregion of mPFC has a permissive role in the extinction of learned fear via enabling extinction-evoked plastic regulation of the excitability of IL neurons. By comparing the expression of different $GABA_AR$ subunits in the mPFC between ES and EF mice, we found that the $GABA_A(\delta)R$ expression was much lower in EF mice than in their ES counterparts and correlated with the ability of the mice to extinguish the learned fear. Global deletion of $GABA_A(\delta)R$ or knocking down its expression in the IL subregion of mPFC led to impaired fear extinction with little influence on fear learning, suggesting a permissive role of the IL $GABA_A(\delta)R$ in fear extinction. Further mechanistic studies revealed that $GABA_A(\delta)R$ deficiency deprived the plastic regulation of the excitability of IL PNs evoked by fear extinction. Finally, re-expressing $GABA_A(\delta)R$ in the IL subregion of KO mice was sufficient to reverse the deficits in both fear extinction and extinction-induced plasticity of neuronal excitability.

As the primary mediator of inhibitory signal in the brain, the $GABA_AR$ family was repetitively shown to suppress fear conditioning. Specifically, systemically administering the benzodiazepines, which potentiate $GABA_AR$ activity, impaired the retention in the inhibitory avoidance and the formation of contextual fear memory (Jensen et al., 1979; Harris and Westbrook, 1998), whereas the administration of $GABA_AR$ antagonist flumazenil was shown to enhance the fear responses in inhibitory avoidance (Izquierdo et al., 1990). Consistently, loss of function of various $GABA_AR$ subtypes including those containing $\alpha1$ (Sonner et al., 2005; Wiltgen et al., 2009), $\alpha2$ (Smith et al., 2012), $\alpha4$ (Moore et al., 2010), and $\gamma2$ (Crestani et al., 1999) significantly promoted fear memory expression. Somewhat surprisingly, we observed that genetic deletion of $GABA_A(\delta)R$ failed to affect the acquisition or retention of fear memory. In line with this, knockdown of $GABA_A(\delta)R$ in neither the IL nor the PL subregion of mPFC influenced the acquisition and expression of fear memory. The exact reasons for the different roles between $GABA_A(\delta)R$ and other $GABA_AR$ members remain unclear but may be associated with their different expression patterns in the brain. It has been shown that in the amygdala and periaqueductal gray, two regions critical for the acquisition and expression of fear memory, the $\alpha1$ and $\alpha2$ subunits are highly expressed (Heldt and Ressler, 2007; Wiltgen et al., 2009; Kasugai et al., 2019). By contrast, the δ-subunit is far less abundant (Peng et al., 2002; Hörtnagl et al., 2013) and may thus have a limited contribution to regulating the neuronal activity in these regions. Of note, evidence also emerged to show that the δ-subunit was involved in the contextual fear learning (Wiltgen et al., 2005; Whissell et al., 2013b) but not the cued fear learning (Wiltgen, 2005; Zhang et al., 2017), raising a possibility that the contribution of δ-subunit in the learning and memory may also vary with the specific paradigm of learning. mPFC is a key region for the extinction of learned fear and increasing studies have been made to reveal the roles of $GABA_AR$ in this region in the regulation of fear extinction (Davis and Myers, 2002; Makkar et al., 2010). First, systematic or local application of muscimol (Disorbo et al., 2009) or benzodiazepines (Bustos et al., 2009; Hart et al., 2009) in IL subregion was shown to impair the fear extinction, and intra-IL infusion of picrotoxin to block GABAergic transmission facilitated fear extinction (McGaugh et al., 1990; Chang and Maren, 2011; Fitzgerald et al., 2014). These data suggest that the $GABA_ARs$, at least in the IL subregion of mPFC, prevent the extinction of learned fear. In sharp contrast, we observed that the $GABA_A(\delta)R$ in IL subregion appeared to facilitate rather than prevent the extinction of learned fear. First, the magnitude of $GABA_A(\delta)R$ current in the IL of individual mice was positively correlated with their ERI. Second, selective knockdown of the $GABA_A(\delta)R$ in IL subregion sufficed to impair the extinction of learned fear, and third, re-expressing $GABA_A(\delta)R$ in the IL subregion of KO mice rescued the deficits of fear extinction. It has been long thought that the limitation of fear extinction and other forms of learning by $GABA_ARs$ is related to their ability to suppress the plastic regulation of glutamatergic transmission in regions engaged in learning and memory. For instance, in amygdala, the $GABA_AR$-mediated inhibition has long been known to prevent long-term potentiation (LTP) of synaptic transmission in both cortical and subcortical afferents to the amygdala and to block fear learning (Manzanares et al., 2005; Wiltgen et al., 2009). In mPFC, blockage of GABAergic inhibition by $GABA_AR$ antagonists also facilitates LTP (Lu et al., 2010; Zhou et al., 2013). However, the effect of the IL $GABA_A(\delta)R$ on fear extinction seems unlikely because of its ability to alter the plasticity of synaptic transmission. In fact, we failed to find any considerable influence of $GABA_A(\delta)R$ KO on extinction-evoked plasticity of glutamatergic transmission in IL neurons. Although the KO mice showed a clear deficit in extinction relative to their WT littermates, the frequency of mEPSCs in the IL neurons of both genotypes was similarly increased following extinction training, and the PPR in the transmission from layer II/III to layer V neurons was also decreased in both. Thus, the plasticity of glutamatergic transmission evoked by extinction remains intact following $GABA_A(\delta)R$ KO and therefore may not explain the resulting deficit of extinction. Instead, we propose that the dysregulation of the intrinsic excitability of IL neurons may be the cause of the defective fear extinction by $GABA_A(\delta)R$ KO. While the extinction training substantially increased the excitability of IL neurons in WT mice, it failed to do so in the KO mice. More importantly, reintroducing $GABA_A(\delta)Rs$ into the IL subregion of KO mice not only restored the defective dynamic of the intrinsic excitability of the IL neurons, but also rescued the loss of extinction in these mice, highlighting an essential contribution of the intrinsic plasticity to fear extinction.

Contrary to the current findings, a recent study by Santini et al. (2008) reported no difference between the naive mice and mice experiencing fear extinction in terms of the neuronal excitability in IL subregion. A possible explanation for this discrepancy may lie in the fact that the neurons recorded in the study by Santini et al. (2008) were from layers II/III and V and those in the current study were only from layer V. Actually, it has been observed that extinction decreased the excitability of IL neurons in layers II/III (Wang et al., 2018). Together with the increased excitability in layer V neurons, as observed in our study, it seems that extinction might have opposite influences on the excitability of IL neurons in layer II/III versus layer V. Thus, if neurons from layers II/III and V were included in the study by Santini et al. (2008), the net effect of extinction might be no change in the excitability of IL neurons.

The $GABA_A(\delta)R$ was repetitively shown to alter the activity of neurons in numerous brain regions, including the cerebellum (Rudolph et al., 2020) and hippocampal dentate gyrus (Maguire et al., 2009). Not surprisingly, we here also observed increased c-*Fos* expression and intrinsic excitability in the IL neurons by

$GABA_A(\delta)$R KO. Based on the findings that extinction training elevated c-*Fos* expression and intrinsic excitability only in the IL neurons of WT mice but not KO mice, we speculate that the increase of neuronal activity following $GABA_A(\delta)$R KO may have a ceiling effect and prevent its further increase by extinction training.

It has been long recognized that fear learning and extinction trigger a spectrum of plastic changes in multiple engaged regions such as hippocampus, amygdala, and mPFC at levels ranging from synaptic transmission and dendritic architecture to neuronal activity (Lai et al., 2012; Kitamura et al., 2017; Liu et al., 2017; Wang et al., 2018; Chen et al., 2020b). While the role of synaptic plasticity in fear learning and extinction has been well documented, increasing attention has also been paid to the participant of the nonsynaptic plasticity. It is now thought that the two forms of plasticity are coordinated to mediate multiple brain functions such as learning and memory (Chen et al., 2020a; Yousuf et al., 2020). The learning of odor-related fear memory was shown to enhance both the postsynaptic potential and neuronal excitability in neurons of lateral amygdala (Rosenkranz and Grace, 2002), and trace fear conditioning increased both the EPSP amplitude and the excitability of dorsal hippocampal neurons (Song et al., 2012). Moreover, fear extinction was also found to alter the glutamatergic transmission and the intrinsic excitability in mPFC neurons (Santini et al., 2008; Pattwell et al., 2012; Bloodgood et al., 2018). Nevertheless, the specific roles of the synaptic versus nonsynaptic plasticity remain incompletely clear. Here, our extinction-deficit model of $GABA_A(\delta)$R KO mice in which the synaptic plasticity remains intact, but the plasticity of excitability becomes defective, may provide an example to highlight a critical role of altered nonsynaptic plasticity per se in learning and memory.

Altogether, our current findings reveal an unconventional and permissive role of $GABA_A(\delta)$R in IL subregion in regulating fear extinction via a nonsynaptic mechanism. Despite this, it remains vague regarding the molecular underlying of the $GABA_A(\delta)$R engagement in the plasticity of neuronal excitability; given the opposite roles played by the $GABA_A(\delta)$R and other $GABA_A$R members in IL subregion in fear extinction, the question is still open about how the different $GABA_A$Rs are coordinated to fine-tune the mPFC-engaged tasks such as fear learning and extinction. Moreover, the expression of $GABA_A(\delta)$R in females was shown to be adaptatively fluctuating following the dynamic changes of sex hormones over the ovarian cycle (Maguire et al., 2005; Maguire and Mody, 2008), making it a little bit tough to identify the exact role of this receptor in females. However, considering the role of $GABA_A(\delta)$Rs in the development of a spectrum of neuropsychological disorders, for example, in postpartum depression (Maguire and Mody, 2008; Barth et al., 2014), whether $GABA_A(\delta)$R also has a role in gating extinction in females as it does in males is still unclear. Future investigations are thus needed to address these issues.

References

Adhikari A, Lerner TN, Finkelstein J, Pak S, Jennings JH, Davidson TJ, Ferenczi E, Gunaydin LA, Mirzabekov JJ, Ye L, Kim S-Y, Lei A, Deisseroth K (2015) Basomedial amygdala mediates top-down control of anxiety and fear. Nature 527:179–185.

Barth AMI, Ferando I, Mody I (2014) Ovarian cycle-linked plasticity of δ-GABAA receptor subunits in hippocampal interneurons affects γ oscillations in vivo. Front Cell Neurosci 8:222.

Bisson JI, Cosgrove S, Lewis C, Robert NP (2015) Post-traumatic stress disorder. BMJ 351:h6161.

Bloodgood DW, Sugam JA, Holmes A, Kash TL (2018) Fear extinction requires infralimbic cortex projections to the basolateral amygdala. Trans Psychiatry 8:60.

Bukalo O, Pinard CR, Holmes A (2014) Mechanisms to medicines: elucidating neural and molecular substrates of fear extinction to identify novel treatments for anxiety disorders. Br J Pharmacol 171:4690–4718.

Burgos-Robles A, Vidal-Gonzalez I, Santini E, Quirk GJ (2007) Consolidation of fear extinction requires NMDA receptor-dependent bursting in the ventromedial prefrontal cortex. Neuron 53:871–880.

Bustos SG, Maldonado H, Molina VA (2009) Disruptive effect of midazolam on fear memory reconsolidation: decisive influence of reactivation time span and memory age. Neuropsychopharmacology 34:446–457.

Chang C, Maren S (2011) Medial prefrontal cortex activation facilitates re-extinction of fear in rats. Learn Mem 18:221–225.

Chen L, Cummings KA, Mau W, Zaki Y, Dong Z, Rabinowitz S, Clem RL, Shuman T, Cai DJ (2020a) The role of intrinsic excitability in the evolution of memory: significance in memory allocation, consolidation, and updating. Neurobiol Learn Mem 173:107266.

Chen W-B, Pan H-Q, He Y, Wang X-H, Zhang W-H, Pan B-X (2020b) Rap1b but not Rap1a in the forebrain is required for learned fear. Cell Biosci 10:107.

Chen Y-H, Hu N-Y, Wu D-Y, Bi L-L, Luo Z-Y, Huang L, Wu J-L, Wang M-L, Li J-T, Song Y-L, Zhang S-R, Jie W, Li X-W, Zhang S-Z, Yang J-M, Gao T-M (2022) PV network plasticity mediated by neuregulin1-ErbB4 signalling controls fear extinction. Mol Psychiatry 27:896–906.

Chhatwal JP, Myers KM, Ressler KJ, Davis M (2005) Regulation of gephyrin and $GABA_A$ receptor binding within the amygdala after fear acquisition and extinction. J Neurosci 25:502–506.

Corcoran KA, Quirk GJ (2007) Activity in prelimbic cortex is necessary for the expression of learned, but not innate, fears. J Neurosci 27:840–844.

Crestani F, Lorez M, Baer K, Essrich C, Benke D, Laurent JP, Belzung C, Fritschy JM, Lüscher B, Mohler H (1999) Decreased GABAA-receptor clustering results in enhanced anxiety and a bias for threat cues. Nat Neurosci 2:833–839.

Davis M, Myers KM (2002) The role of glutamate and gamma-aminobutyric acid in fear extinction: clinical implications for exposure therapy. Biol Psychiatry 52:998–1007.

Disorbo A, Wilson GN, Bacik S, Hoxha Z, Biada JM, Mickley GA (2009) Time-dependent retrograde amnesic effects of muscimol on conditioned taste aversion extinction. Pharmacol Biochem Behav 92:319–326.

Etkin A, Egner T, Kalisch R (2011) Emotional processing in anterior cingulate and medial prefrontal cortex. Trends Cogn Sci 15:85–93.

Fitzgerald PJ, Whittle N, Flynn SM, Graybeal C, Pinard CR, Gunduz-Cinar O, Kravitz AV, Singewald N, Holmes A (2014) Prefrontal single-unit firing associated with deficient extinction in mice. Neurobiol Learn Mem 113:69–81.

Flavell SW, Greenberg ME (2008) Signaling mechanisms linking neuronal activity to gene expression and plasticity of the nervous system. Annu Rev Neurosci 31:563–590.

Giustino TF, Maren S (2015) The role of the medial prefrontal cortex in the conditioning and extinction of fear. Front Behav Neurosci 9:298.

Harris JA, Westbrook RF (1998) Benzodiazepine-induced amnesia in rats: reinstatement of conditioned performance by noxious stimulation on test. Behav Neurosci 112:183–192.

Hart G, Harris JA, Westbrook RF (2009) Systemic or intra-amygdala injection of a benzodiazepine (midazolam) impairs extinction but spares re-extinction of conditioned fear responses. Learn Mem 16:53–61.

Heldt SA, Ressler KJ (2007) Forebrain and midbrain distribution of major benzodiazepine-sensitive GABAA receptor subunits in the adult C57 mouse as assessed with in situ hybridization. Neuroscience 150:370–385.

Hörtnagl H, Tasan RO, Wieselthaler A, Kirchmair E, Sieghart W, Sperk G (2013) Patterns of mRNA and protein expression for 12 GABAA receptor subunits in the mouse brain. Neuroscience 236:345–372.

Izquierdo I, Pereira ME, Medina JH (1990) Benzodiazepine receptor ligand influences on acquisition: suggestion of an endogenous modulatory mechanism mediated by benzodiazepine receptors. Behav Neural Biol 54:27–41.

Jensen RA, Martinez JL, Vasquez BJ, McGaugh JL (1979) Benzodiazepines alter acquisition and retention of an inhibitory avoidance response in mice. Psychopharmacology (Berl) 64:125–126.

Kasugai Y, Vogel E, Hörtnagl H, Schönherr S, Paradiso E, Hauschild M, Göbel G, Milenkovic I, Peterschmitt Y, Tasan R, Sperk G, Shigemoto R, Sieghart W, Singewald N, Lüthi A, Ferraguti F (2019) Structural and functional remodeling of amygdala GABAergic synapses in associative fear learning. Neuron 104:781–794.e4.

Kitamura T, Ogawa SK, Roy DS, Okuyama T, Morrissey MD, Smith LM, Redondo RL, Tonegawa S (2017) Engrams and circuits crucial for systems consolidation of a memory. Science 356:73–78.

Lai CSW, Franke TF, Gan W-B (2012) Opposite effects of fear conditioning and extinction on dendritic spine remodelling. Nature 483:87–91.

Liu W-Z, Zhang W-H, Zheng Z-H, Zou J-X, Liu X-X, Huang S-H, You W-J, He Y, Zhang J-Y, Wang X-D, Pan B-X (2020) Identification of a prefrontal cortex-to-amygdala pathway for chronic stress-induced anxiety. Nat Commun 11:2221.

Liu Z-P, He Q-H, Pan H-Q, Xu X-B, Chen W-B, He Y, Zhou J, Zhang W-H, Zhang J-Y, Ying X-P, Han R-W, Li B-M, Gao T-M, Pan B-X (2017) Delta subunit-containing gamma-aminobutyric acid a receptor disinhibits lateral amygdala and facilitates fear expression in mice. Biol Psychiatry 81:990–1002.

Lu H, Cheng P, Lim BK, Khoshnevisrad N, Poo M (2010) Elevated BDNF after cocaine withdrawal facilitates LTP in medial prefrontal cortex by suppressing GABA inhibition. Neuron 67:821–833.

Maguire J, Mody I (2008) $GABA_AR$ plasticity during pregnancy: relevance to postpartum depression. Neuron 59:207–213.

Maguire J, Ferando I, Simonsen C, Mody I (2009) Excitability changes related to $GABA_A$ receptor plasticity during pregnancy. J Neurosci 29:9592–9601.

Maguire JL, Stell BM, Rafizadeh M, Mody I (2005) Ovarian cycle–linked changes in $GABA_A$ receptors mediating tonic inhibition alter seizure susceptibility and anxiety. Nat Neurosci 8:797–804.

Makkar SR, Zhang SQ, Cranney J (2010) Behavioral and neural analysis of GABA in the acquisition, consolidation, reconsolidation, and extinction of fear memory. Neuropsychopharmacology 35:1625–1652.

Manzanares PAR, Isoardi NA, Carrer HF, Molina VA (2005) Previous stress facilitates fear memory, attenuates GABAergic inhibition, and increases synaptic plasticity in the rat basolateral amygdala. J Neurosci 25:8725–8734.

Marek R, Jin J, Goode TD, Giustino TF, Wang Q, Acca GM, Holehonnur R, Ploski JE, Fitzgerald PJ, Lynagh T, Lynch JW, Maren S, Sah P (2018a) Hippocampus-driven feed-forward inhibition of the prefrontal cortex mediates relapse of extinguished fear. Nat Neurosci 21:384–392.

Marek R, Xu L, Sullivan RKP, Sah P (2018b) Excitatory connections between the prelimbic and infralimbic medial prefrontal cortex show a role for the prelimbic cortex in fear extinction. Nat Neurosci 21:654–658.

McGaugh JL, Castellano C, Brioni J (1990) Picrotoxin enhances latent extinction of conditioned fear. Behav Neurosci 104:264–267.

Milad MR, Quirk GJ (2002) Neurons in medial prefrontal cortex signal memory for fear extinction. Nature 420:70–74.

Milad MR, Wright CI, Orr SP, Pitman RK, Quirk GJ, Rauch SL (2007) Recall of fear extinction in humans activates the ventromedial prefrontal cortex and hippocampus in concert. Biol Psychiatry 62:446–454.

Milad MR, Orr SP, Lasko NB, Chang Y, Rauch SL, Pitman RK (2008) Presence and acquired origin of reduced recall for fear extinction in PTSD: results of a twin study. J Psychiatr Res 42:515–520.

Milad MR, Pitman RK, Ellis CB, Gold AL, Shin LM, Lasko NB, Zeidan MA, Handwerger K, Orr SP, Rauch SL (2009) Neurobiological basis of failure to recall extinction memory in posttraumatic stress disorder. Biol Psychiatry 66:1075–1082.

Moore MD, Cushman J, Chandra D, Homanics GE, Olsen RW, Fanselow MS (2010) Trace and contextual fear conditioning is enhanced in mice lacking the $\alpha 4$ subunit of the $GABA_A$ receptor. Neurobiol Learn Mem 93:383–387.

Morgan MA, Romanski LM, LeDoux JE (1993) Extinction of emotional learning: contribution of medial prefrontal cortex. Neurosci Lett 163:109–113.

Myers KM, Davis M (2007) Mechanisms of fear extinction. Mol Psychiatry 12:120–150.

Pan H-Q, Zhang W-H, Liao C-Z, He Y, Xiao Z-M, Qin X, Liu W-Z, Wang N, Zou J-X, Liu X-X, Pan B-X (2020) Chronic stress oppositely regulates tonic inhibition in Thy1-expressing and non-expressing neurons in amygdala. Front Neurosci 14:299.

Pape H-C, Pare D (2010) Plastic synaptic networks of the amygdala for the acquisition, expression, and extinction of conditioned fear. Physiol Rev 90:419–463.

Pattwell SS, Duhoux S, Hartley CA, Johnson DC, Jing D, Elliott MD, Ruberry EJ, Powers A, Mehta N, Yang RR, Soliman F, Glatt CE, Casey BJ, Ninan I, Lee FS (2012) Altered fear learning across development in both mouse and human. Proc Natl Acad Sci U|S|A 109:16318–16323.

Peng Z, Hauer B, Mihalek RM, Homanics GE, Sieghart W, Olsen RW, Houser CR (2002) $GABA_A$ receptor changes in δ subunit-deficient mice: altered expression of $\alpha 4$ and $\gamma 2$ subunits in the forebrain. J Comp Neurol 446:179–197.

Peters J, Dieppa-Perea LM, Melendez LM, Quirk GJ (2010) Induction of fear extinction with hippocampal-infralimbic BDNF. Science 328:1288–1290.

Qin X, Pan H-Q, Huang S-H, Zou J-X, Zheng Z-H, Liu X-X, You W-J, Liu Z-P, Cao J-L, Zhang W-H, Pan B-X (2022) $GABA_A(\delta)$ receptor hypofunction in the amygdala-hippocampal circuit underlies stress-induced anxiety. Sci Bull 67:97–110.

Quirk GJ, Russo GK, Barron JL, Lebron K (2000) The role of ventromedial prefrontal cortex in the recovery of extinguished fear. J Neurosci 20:6225–6231.

Rosenkranz JA, Grace AA (2002) Dopamine-mediated modulation of odour-evoked amygdala potentials during pavlovian conditioning. Nature 417:282–287.

Rudolph S, Guo C, Pashkovski SL, Osorno T, Gillis WF, Krauss JM, Nyitrai H, Flaquer I, El-Rifai M, Datta SR, Regehr WG (2020) Cerebellum-specific deletion of the GABAA receptor δ subunit leads to sex-specific disruption of behavior. Cell Rep 33:108338.

Santini E, Quirk GJ, Porter JT (2008) Fear conditioning and extinction differentially modify the intrinsic excitability of infralimbic neurons. J Neurosci 28:4028–4036.

Sierra-Mercado D, Padilla-Coreano N, Quirk GJ (2011) Dissociable roles of prelimbic and infralimbic cortices, ventral hippocampus, and basolateral amygdala in the expression and extinction of conditioned fear. Neuropsychopharmacology 36:529–538.

Singewald N, Schmuckermair C, Whittle N, Holmes A, Ressler KJ (2015) Pharmacology of cognitive enhancers for exposure-based therapy of fear, anxiety and trauma-related disorders. Pharmacol Ther 149:150–190.

Smith KS, Engin E, Meloni EG, Rudolph U (2012) Benzodiazepine-induced anxiolysis and reduction of conditioned fear are mediated by distinct GABAA receptor subtypes in mice. Neuropharmacology 63:250–258.

Song C, Detert JA, Sehgal M, Moyer JR (2012) Trace fear conditioning enhances synaptic and intrinsic plasticity in rat hippocampus. J Neurophysiol 107:3397–3408.

Sonner JM, Cascio M, Xing Y, Fanselow MS, Kralic JE, Morrow AL, Korpi ER, Hardy S, Sloat B, Eger EI, Homanics GE (2005) $\alpha 1$ subunit-containing GABA type A receptors in forebrain contribute to the effect of inhaled anesthetics on conditioned fear. Mol Pharmacol 68:61–68.

Tovote P, Fadok JP, Lüthi A (2015) Neuronal circuits for fear and anxiety. Nat Rev Neurosci 16:317–331.

Wang Q, Wang Q, Song X-L, Jiang Q, Wu Y-J, Li Y, Yuan T-F, Zhang S, Xu N-J, Zhu MX, Li W-G, Xu T-L (2018) Fear extinction requires ASIC1a-dependent regulation of hippocampal-prefrontal correlates. Sci Adv 4:eaau3075.

Whissell PD, Eng D, Lecker I, Wang D-S, Martin LJ, Orser BA (2013a) Acutely increasing δGABAA receptor activity impairs memory and inhibits synaptic plasticity in the hippocampus. Front Neural Circuits 7:146.

Whissell PD, Rosenzweig S, Lecker I, Wang D-S, Wojtowicz JM, Orser BA (2013b) γ-aminobutyric acid type A receptors that contain the δ subunit promote memory and neurogenesis in the dentate gyrus. Ann Neurol 74:611–621.

Whissell PD, Lecker I, Wang D-S, Yu J, Orser BA (2015) Altered expression of $\delta GABA_A$ receptors in health and disease. Neuropharmacology 88:24–35.

Wiltgen BJ, Sanders MJ, Ferguson C, Homanics GE, Fanselow MS (2005) Trace fear conditioning is enhanced in mice lacking the subunit of the $GABA_A$ receptor. Learn Mem 12:327–333.

Wiltgen BJ, Godsil B, Peng Z, Saab F, June H, Van Linn ML, Cook JM, Houser C, O'dell T, Homanics GE, Fanselow M (2009) The $\alpha 1$ subunit of

the GABA(A) receptor modulates fear learning and plasticity in the lateral amygdala. Front Behav Neurosci 3:37.

Yousuf H, Ehlers VL, Sehgal M, Song C, Moyer JR (2020) Modulation of intrinsic excitability as a function of learning within the fear conditioning circuit. Neurobiol Learn Mem 167:107132.

Zhang W-H, Zhou J, Pan H-Q, Wang X-Y, Liu W-Z, Zhang J-Y, Yin X-P, Pan B-X (2017) δ Subunit-containing GABAA receptor prevents overgeneralization of fear in adult mice. Learn Mem 24:381–384.

Zhang W-H, Liu W-Z, He Y, You W-J, Zhang J-Y, Xu H, Tian X-L, Li B-M, Mei L, Holmes A, Pan B-X (2019) Chronic stress causes projection-specific adaptation of amygdala neurons via small-conductance calcium-activated potassium channel downregulation. Biol Psychiatry 85:812–828.

Zheng Z-H, Tu J-L, Li X-H, Hua Q, Liu W-Z, Liu Y, Pan B-X, Hu P, Zhang W-H (2021) Neuroinflammation induces anxiety- and depressive-like behavior by modulating neuronal plasticity in the basolateral amygdala. Brain Behav Immun 91:505–518.

Zhou H-C, Sun Y-Y, Cai W, He X-T, Yi F, Li B-M, Zhang X-H (2013) Activation of β2-adrenoceptor enhances synaptic potentiation and behavioral memory via cAMP-PKA signaling in the medial prefrontal cortex of rats. Learn Mem 20:274–284.